NuRD chromatin remodeling is required to repair exogenous DSBs in the *Caenorhabditis elegans* germline

Deepshikha Ananthaswamy[1], Kelin Funes[1†], Thiago Borges[1†], Scott Roques[1], Nina Fassnacht[2], Sereen El Jamal[2], Paula M. Checchi[2], Teresa Wei-sy Lee[1]*

[1] Department of Biological Sciences, University of Massachusetts Lowell, 198 Riverside Dr. Lowell MA, 01854

[2] Department of Biology, Marist College, 3399 North Road, Poughkeepsie, NY 12601

† contributed equally

* for correspondence, teresa_lee@uml.edu

Running title: NuRD remodeling repairs germline exogenous DSBs

Keywords: DNA repair, NuRD (nucleosome remodeling and deacetylase complex), LET-418/CHD4, FCD-2/FANCD2, germline

ABSTRACT

Organisms rely on coordinated networks of DNA repair pathways to protect genomes against toxic double-strand breaks (DSBs), particularly in germ cells. All repair mechanisms must successfully negotiate the local chromatin environment in order to access DNA. For example, nucleosomes can be repositioned by the highly conserved Nucleosome Remodeling and Deacetylase (NuRD) complex. In *Caenorhabditis elegans*, NuRD functions in the germline to repair DSBs – the loss of NuRD's ATPase subunit, LET-418/CHD4, prevents DSB resolution and therefore reduces fertility. In this study, we challenge germlines with exogenous DNA damage to better understand NuRD's role in repairing DSBs. We find that *let-418* mutants are hypersensitive to cisplatin and hydroxyurea: exposure to either mutagen impedes DSB repair, generates aneuploid oocytes, and severely reduces fertility and embryonic survival. These defects resemble those seen when the Fanconi anemia (FA) DNA repair pathway is compromised, and we find that LET-418's activity is epistatic to that of the FA component FCD-2/FANCD2. We propose a model in which NuRD is recruited to the site of DNA lesions to remodel chromatin and allow access for FA pathway components. Together, these results implicate NuRD in the repair of both endogenous DSBs and exogenous DNA lesions to preserve genome integrity in developing germ cells.

ARTICLE SUMMARY

Preserving genome integrity in germ cells is critical for the survival of individuals and species. Our previous work shows that nucleosome remodeling plays an important role in repairing meiotic DNA damage. Here, we further challenge genomes with toxic DNA damaging agents to test the requirement for remodeling in the germline. We find that DNA damage accumulates in the absence of remodeling, which drastically reduces oocyte quality, and also show that the requirement for remodeling is epistatic to the Fanconi anemia DNA repair pathway. These findings demonstrate that local chromatin environments must be remodeled in response to DNA damage to maintain oocyte quality.

INTRODUCTION

DNA damage poses a danger to all cells, but if left unrepaired in germ cells, it can prove deleterious for organismal fitness. During meiosis, any DNA lesion that persists until chromosome segregation will generate an aneuploid gamete, which in turn causes infertility or embryonic lethality (Ceccaldi et al., 2016; Kim et al., 2016). The evolutionary pressure to protect genomes for future generations has generated multiple distinct, but overlapping, DNA repair pathways. These pathways handle both endogenous programmed double-strand breaks (DSBs) required for crossover recombination, along with any exogenous DNA damage incurred in the germline (Chapman et al., 2012; Gartner and Engebrecht, 2022; Keeney, 2007). Studies in organisms ranging from budding yeast to mammals have identified strong conservation among these repair pathways, which include error-free mechanisms like homologous recombination and error-prone mechanisms like non-homologous end joining (De Massy, 2013; Stinson and Loparo, 2021, 2021; Wilson et al., 1997). For example, the Fanconi anemia (FA) pathway is activated when replication forks collide with DNA interstrand crosslinks, which are one of the most toxic DNA lesions (Gartner and Engebrecht, 2022). Components of the FA pathway coordinate the excision of the crosslink and conversion to DSBs, which can then be resolved by the meiotic homologous recombination pathway (Adamo et al., 2010; Lachaud et al., 2016; Raghunandan et al., 2015; Schlacher et al., 2012). Defects in the FA pathway are linked to an elevated risk of cancer and cause chromosomal instability or meiotic catastrophe, hallmarks of the rare congenital disorder of Fanconi anemia (Auerbach, 2009, 1993; Ceccaldi et al., 2016; De Winter and Joenje, 2009; Nalepa and Clapp, 2018; Tischkowitz et al., 2003, 2004).

In eukaryotes, DNA repair must always happen in the context of chromatin, where DNA is wrapped around histone octamers to form nucleosomes (Allis and Jenuwein, 2016). Nucleosomes act as obstacles that control access to DNA, and therefore their spacing is regulated by nucleosome remodeling complexes (Becker and Workman, 2013). The highly conserved remodeling complex, Nucleosome remodeling and deacetylase (NuRD), includes ATPase remodelers from the chromodomain helicase DNA binding (CHD) family (Basta and Rauchman, 2015; Kehle, 1998; Tong et al., 1998; Wade et al., 1998; Woodage et al., 1997; Xue et al., 1998). In addition to CHD remodeling subunits, NuRD also consists of the histone deacetylases HDAC1/2, histone demethylase LSD1/KDM1A, and other components that allow NuRD to bind modified histones, methyl CpG, and other proteins (Basta and Rauchman, 2015; Wang et al., 2009; Whyte et al., 2012). Initially, NuRD's primary role was thought to be transcriptional repression; but studies have since identified a more nuanced involvement in gene expression, along with other biological functions like DNA repair (Basta and Rauchman, 2015). The

59 nematode *Caenorhabditis elegans* has two catalytic CHD paralogs associated with the core NuRD
60 complex: CHD-3 (also known as Mi-2α or CHD3 in mammals) and LET-418 (Mi-2β or CHD4) (Passannante
61 et al., 2010; von Zelewsky et al., 2000). Mutations in either the *chd-3* or the *let-418* genes severely
62 reduce fertility due to high levels of persistent meiotic DSBs, (McMurchy et al., 2017; Turcotte et al.,
63 2018).
64 These studies highlight the importance of NuRD's role in the germline for proper DNA repair –
65 the loss of NuRD activity appears to shunt DSBs from error-free repair towards error-prone pathways
66 like NHEJ. The genomic instability of *chd-3* or *let-418* mutants resembles those seen in mutants
67 defective for the FA pathway (Rageul and Kim, 2020; Tsui and Crismani, 2019). One hallmark of
68 mutations in FA components is an increased sensitivity to mutagens like cisplatin, which induces DNA
69 interstrand crosslinks, or hydroxyurea, which stalls replication forks (Bailly and Gartner, 2011; Datta and
70 Brosh Jr., 2019; Youds et al., 2009). Both of these lesions can generate DSBs if left unrepaired, which
71 activate the S-phase checkpoint and subsequently delays cell cycle progression (Kessler and Yanowitz,
72 2014; Kim and Colaiácovo, 2015). Resolution of interstrand crosslinks by the FA pathway involves
73 recognition and binding by the core FA complex, which then recruits FANCD2 to chromatin by mono-
74 ubiquitination (Nakanishi et al., 2005; Niraj et al., 2019). Once at the DNA lesion, FANCD2 orchestrates
75 the repair of the lesion by converting it to DSBs, which are then resolved by homologous recombination
76 (Ceccaldi et al., 2016; Niraj et al., 2019).
77 NuRD is required for repairing DNA lesions in germ cells (McMurchy et al., 2017; Turcotte et al.,
78 2018), but it is not clear how or whether nucleosome remodeling interacts with repair processes like the
79 FA pathway. Here, we challenge the germline by inducing exogenous DNA damage to investigate the
80 relationship between the FA pathway and NuRD's catalytic component, LET-418/CHD4. *C. elegans* has
81 homologs for many core FA components, including FCD-2/FANCD2 (Kim et al., 2018; Lee et al., 2010).
82 One advantage of using *C. elegans* for this study is the germline's spatiotemporal organization, which
83 allows us to easily follow the effects of mutagen exposure at multiple downstream stages during
84 oogenesis (Jaramillo-Lambert et al., 2007; Kessler and Yanowitz, 2014). We show that LET-418 activity is
85 epistatic to FCD-2 and is necessary to repair germline DSBs and preserve fertility. These results support a
86 model where NuRD generates a permissive local chromatin environment at the site of DNA damage to
87 allow access to DSB repair machinery and therefore preserve gamete quality in the face of genotoxic
88 stress.
89
90 **METHODS**

91 Strains and husbandry: All strains were cultured using standard methods (Brenner, 1974) at 20°C on 6-
92 cm NGM agar plates spotted with OP50 *E. coli* grown overnight at 37°C in Luria Broth (LB). The *syb6818*
93 allele is a deletion of LET-418's ATPase domain and removes amino acids 590-1114. The *syb6708* allele is
94 a deletion of LET-418's PHD finger domain and removes amino acids 256-365. Both domains were
95 identified using an NCBI structure prediction and based on homology with human CHD4 (Farnung et al.,
96 2020; Sayers et al., 2022). Sterile strains were maintained over an *nT1* balancer chromosome by picking
97 GFP-positive heterozygotes. The following strains were obtained from the *Caenorhabditis* Genetics
98 Center or were generated by SunyBiotech (*syb* alleles, which were backcrossed five times to N2):
99 - N2: wild-type (Bristol isolate)
100 - MT14390: *let-418 (n3536) V*
101 - NB105: *fcd-2 (tm1298) IV*
102 - TG1660: *xpf-1 (tm2842) II*
103 - TER14: *fcd-2 (tm1298) IV; let-418 (n3536) V*
104 - TER6: *let-418 (syb6818)/nT1 [qls51] IV:V*
105 - TER10: *let-418 (syb6708) V*
106
107 Mutagen exposure: All exposure assays were performed on hermaphrodites cultured at 20°C on 3-cm
108 NGM agar plates. Plates were first spotted with OP50 *E. coli*, then treated by spreading 250 µL of either
109 400 µM cisplatin (Sigma Aldrich) or 10 mM hydroxyurea (Thermo Scientific) onto agar at least 12 hours
110 prior to experiment. Synchronized young adult hermaphrodites (12 hours post-L4 larval stage) were
111 placed on mutagen plates for 24 hours, then moved to regular NGM plates to recover before assessing
112 nuclei in the appropriate meiotic stage (timing for each assay described below) (Jaramillo-Lambert et al.,
113 2007; Kessler and Yanowitz, 2014).
114
115 Immunofluorescence and image processing: Following exposure to cisplatin or hydroxyurea,
116 hermaphrodites were allowed to recover on NGM plates for four hours to produce better gonad
117 extrusion. Gonad dissection, fixation, and immunostaining were performed as previously described
118 (Ananthaswamy et al., 2022). In brief, gonads were dissected using 25-gauge syringe needles, fixed in
119 0.8% paraformaldehyde (Electron Microscopy Services) for five minutes at room temperature, subjected
120 to freeze crack, and dehydrated in 100% methanol for one minute at -20°C. Slides were washed 3X with
121 PBS + 0.1% Tween-20 (Thermo Scientific) prior to overnight incubation at room temperature with
122 primary antibody. Slides were washed three times before incubation with secondary antibody for four

123 hours at room temperature. Samples were mounted in VectaShield (Vector Laboratories) with 2 µg/ml
124 DAPI (Thermo Life) before sealing with nail polish. Antibodies used were rabbit anti-RAD-51 at 1:5000
125 (gifted by Diana Libuda, (Kurhanewicz et al., 2020)) and donkey anti-rabbit AlexaFluor594 at 1:400
126 (Invitrogen).
127 Immunofluorescence images were collected at 63x as Z-stacks with 0.25 µm intervals using a
128 Zeiss Axio Imager M2 microscope with Zen 3.8 software (Zeiss). All representative images shown are
129 max projections after processing in FIJI software (Schindelin et al., 2012). Raw z-stacks were used to
130 quantify RAD-51 foci. Three biological replicates were performed, with five gonads imaged per condition
131 in each replicate (each condition had a total of 15 gonads analyzed). Only one gonad arm was analyzed
132 from each hermaphrodite. All statistical analyses were performed in Prism 8 (GraphPad), with p-values
133 determined using a Kruskal-Wallis test with Dunn's post-hoc test.
134
135 Analysis of diakinesis DAPI bodies: Following exposure to cisplatin or hydroxyurea, hermaphrodites were
136 allowed to recover for 60 hours, which is the time required for a mitotic oocyte nucleus to progress
137 through meiosis to diakinesis. Gonads were dissected as previously described (Ananthaswamy et al.,
138 2022) with the following modifications: the primary and secondary antibody incubation steps were
139 skipped, and slides were washed at least three times in PBS + 0.1% Tween-20 (Thermo Scientific) before
140 mounting in SlowFade Diamond (Molecular Probes) with 2 µg/ml DAPI (Thermo Life). Images were
141 collected at 63x as Z-stacks with 0.25 µm intervals captured on Zeiss Axio Imager M2 using Zen 3.8
142 software (Zeiss). All representative images shown are max projections after processing in FIJI (Schindelin
143 et al., 2012). Raw z-stacks were used to quantify DAPI-stained bodies in the -1 to the -4 oocyte from the
144 spermatheca. Three biological replicates were performed, with each condition consisting of a minimum
145 of 100 nuclei from >27 hermaphrodites. P-values were determined using a Fisher's exact test.
146
147 Embryonic survival – 4-hr laying period: After exposure to cisplatin, hydroxyurea, or nitrogen mustard,
148 hermaphrodites were allowed to recover on NGM plates for 60 hours, which is the length of time for
149 mitotic oocyte nuclei to progress through the gonad and be laid as fertilized embryos. Exposed mothers
150 were then moved onto freshly spotted 3-cm NGM plates (five to ten per plate) and allowed to lay for
151 four hours before being removed from plates. The number of embryos per plate was immediately
152 recorded after removal of mothers, and were scored as fertilized, unfertilized, or dead. Hatched progeny
153 were counted as adults three days later. Percent survival was calculated by dividing the number of
154 hatched progeny by the number of embryos, multiplied by 100. Each condition consists of progeny from

155 125-150 mothers, collected over three biological replicates. All statistical analyses were performed in
156 Prism 8 (GraphPad), with p-values determined from a one-way ANOVA after a Šídák correction used to
157 account for multiple comparisons.
158
159 Embryonic survival – entire brood: Individual hermaphrodites were isolated on separate plates as L4
160 larvae and transferred every 12 hours until the end of their fertile period (usually 5-6 days). Embryos
161 and unfertilized eggs were counted every 12 hours immediately after transfer of the mother. Total
162 brood was calculated for each mother as all embryos laid during the fertile period. Hatched progeny
163 were then counted two to three days later (when they were L4s or young adults). Percent survival was
164 calculated by dividing the number of hatched progeny by the number of embryos laid and multiplied by
165 100. Each biological replicate includes the broods of five mothers scored for each genotype (i.e. five
166 technical replicates). The following biological replicates were performed: seven of N2; six of *let-418*
167 *(n3536)*; four of *let-418 (syb6818)*; and one of *let-418 (syb6708)*. Broods were censored from analysis if
168 the mother died of unnatural causes before the end of their fertile period (usually from vulva rupture or
169 crawling off the agar). All statistical analyses were performed in Prism 8 (GraphPad), with p-values
170 determined from a one-way ANOVA after a Šídák correction used to account for multiple comparisons.
171
172 **RESULTS**
173 LET-418 activity is required to repair mitotic DNA lesions.
174 Mutants lacking both NuRD paralogs (CHD3 and CHD4) have severely compromised fertility,
175 making downstream analysis difficult (Turcotte et al., 2018). Therefore, we focused only on the impact
176 of LET-418/CHD4, reasoning that it plays a larger role in repairing germline DSBs because its loss causes
177 more meiotic defects than that of CHD-3 (Turcotte et al., 2018). At pachytene entry, *let-418* mutants
178 have significantly more DSBs than wild-type (Turcotte et al., 2018), leading us to wonder whether these
179 DSBs represent unrepaired DNA damage acquired during replication. We used cisplatin and hydroxyurea
180 to generate exogenous DNA damage in *let-418 (n3536)* missense mutants and *fcd-2 (tm1298)* deletion
181 mutants, which lack the FA pathway component FCD-2/FANCD2. We capitalized on the fact that the *C.*
182 *elegans* germline is organized in a spatiotemporal manner, with nuclei undergoing mitosis at the distal
183 tip and moving proximally as they proceed through meiosis. The timing of how nuclei progress through
184 mitotic replication, meiosis, oocyte maturation, and fertilization has been extensively characterized
185 (Jaramillo-Lambert et al., 2007; Kessler and Yanowitz, 2014). We therefore estimated the timing post
186 exposure to capture the impact of DNA damage incurred during mitosis.

187 Mitotic zone DSBs were assessed using an antibody for the RecA recombinase RAD-51, a
188 common cytological marker (Alpi et al., 2003; Colaiácovo et al., 2003; Kurhanewicz et al., 2020).
189 Hermaphrodites were cultured on either cisplatin or hydroxyurea for twenty hours, allowed to recover
190 for four hours, and dissected for immunofluorescence (Jaramillo-Lambert et al., 2007; Kessler and
191 Yanowitz, 2014). Consistent with prior reports, unexposed wild-type animals accumulated few RAD-51
192 foci in the mitotic zone (Fig. 1A, C, Fig. 2A, C, and Table S1) (Alpi et al., 2003; Turcotte et al., 2018), which
193 was also true for all mutants examined, with foci in less than 8% of nuclei. Unexposed *let-418* single
194 mutants had a modest but significant increase in foci compared to wild-type animals ($P < 0.0001$,
195 Kruskal-Wallis test), but neither *fcd-2* single mutants nor *fcd-2; let-418* double mutants had more foci
196 than wild-type (Fig. 1A, $P > 0.08$ for both comparisons, Kruskal-Wallis test). Unexposed *fcd-2; let-418*
197 double mutants were not more affected than either single mutant ($P > 0.8$ for both comparisons,
198 Kruskal-Wallis test). We note that, although average foci number did not vary much between genotypes,
199 we occasionally observed nuclei with two or three foci in *let-418* single mutants (0.8% of nuclei) and *fcd-*
200 *2; let-418* double mutants (0.7%), which were rarely seen in wild-type germlines (0.2%) (Fig. 1A and
201 Table S1).
202 As expected, exposure to 400 µM cisplatin raised RAD-51 focus number across all genotypes
203 compared to unexposed controls (Fig. 1B, D and Table S1). This dose was chosen based on a dose curve
204 showing that 400 µM significantly impacted embryonic survival in both wild-type and mutant
205 populations (Fig. S2). Wild-type populations exposed to cisplatin accumulated over five times more foci
206 than their unexposed controls $P < 0.0001$, Kruskal-Wallis test) (Fig. 1A, B). Similarly, both exposed *fcd-2*
207 and *let-418* mutants accumulated five times more foci than unexposed controls ($P < 0.0001$ for both
208 comparisons, Kruskal-Wallis test) (Fig. 1A, B). In *let-418* mutants, the increase was driven by nuclei with
209 multiple foci, sometimes as many as five (10.8% of nuclei compared to 0.7%). Interestingly, exposed *fcd-*
210 *2; let-418* double mutants strongly resembled exposed *let-418* single mutants, with over seven times
211 more foci than unexposed controls ($P < 0.0001$, Kruskal-Wallis test) (Fig. 1B). Again, this large increase
212 was primarily driven by nuclei with multiple foci, especially those with four or five (9.6% of nuclei
213 compared to 0.7%). Notably, nuclei with four or five foci were never observed in exposed wild-type or
214 *fcd-2* single mutants.
215 We next challenged mutants using hydroxyurea, which stalls replication forks and generates
216 DSBs if left unrepaired (Bailly and Gartner, 2011). A dose of 10 mM was chosen after examining
217 embryonic survival in wild-type and *let-418* mutants across a dose curve (Fig. S3 and Table S5).
218 Hydroxyurea affected all genotypes in a manner similar to cisplatin (Fig. 2 and Table S1). Once again, few

219 DSBs were observed in each unexposed population, with less than 7% of mitotic nuclei containing a
220 RAD-51 focus (Fig. 2A). As expected, exposure to hydroxyurea raised the average number of foci in all
221 genotypes ($P < 0.02$ for all comparisons, Kruskal-Wallis test) (Fig. 2B). Exposed wild-type populations and
222 *fcd-2* mutants had nearly two times more foci than unexposed controls ($P < 0.02$ for both comparisons,
223 Kruskal-Wallis test), both primarily driven by an increase in the number of nuclei with one focus.
224 Resembling what we observed after cisplatin exposure, *let-418* single mutants and *fcd-2; let-418* double
225 mutants responded to hydroxyurea in similar ways (Fig. 2B, D). Both mutants had two times more foci
226 than unexposed controls ($P < 0.0001$ for both comparisons, Kruskal-Wallis test). We note that exposed
227 *let-418* and *fcd-2; let-418* mutants each contained nuclei with as many as five RAD-51 foci, which were
228 almost never observed in wild-type or *fcd-2* mutant populations (Fig. 2B). Taken together, these data
229 show how exposure to cisplatin or hydroxyurea generates DNA lesions that require the activity of the
230 *let-418* gene and the *fcd-2* gene for proper repair. Additionally, *fcd-2; let-418* double mutants
231 phenocopy *let-418* single mutants when responding to mitotic DNA damage in the germline.
232
233 <u>Unrepaired mitotic DSBs affect oocyte quality in *let-418* mutants.</u>
234 Although *let-418* single mutants accumulate DSBs in the mitotic region and during pachytene,
235 they do not display aneuploidy or chromosome fragmentation, indicating that any remaining DSBs are
236 fully resolved by diakinesis (Turcotte et al., 2018). However, mutants lacking both CHD paralogs, CHD-3
237 and LET-418, suffer from meiotic catastrophe, genome fragmentation, and chromosome fusions
238 (Turcotte et al., 2018), suggesting that NuRD needs at least one CHD component to repair endogenous
239 DSBs. To see whether LET-418 is required for the resolution of exogenous DNA lesions, we exposed
240 hermaphrodites to cisplatin or hydroxyurea for twenty hours and allowed them to recover for sixty
241 hours (Jaramillo-Lambert et al., 2007; Kessler and Yanowitz, 2014). This timing allows us to induce DNA
242 damage in mitotic cells and assess its impact during diakinesis, where we expect to see six DAPI-staining
243 bodies, one for each homologous pair of chromosomes.
244 As expected, unexposed wild-type animals rarely produced aneuploid gametes: when scoring
245 aged mothers in their third day of adulthood, we found that only 9% of oocytes contained five DAPI-
246 stained bivalents (Fig. 3A, C, E, Fig. S1, and Table S2). This result is consistent with previous studies
247 showing that oocyte quality decreases with maternal age (Achache et al., 2021; Andux and Ellis, 2008;
248 Luo et al., 2010; Scharf et al., 2021). Each unexposed mutant produced more aneuploid oocytes than
249 wild-type controls, with at least 16% of nuclei containing fewer than six DAPI bodies ($P < 0.01$ for all
250 comparisons, Fisher's exact test), including oocytes with four DAPI bodies that were never observed in

251 wild-type animals (Fig. 3A, C, E and Fig. S1). We also noted that *let-418* single mutants generated a rare
252 oocyte with seven DAPI bodies (Fig. 3E). The presence of univalents in this nucleus reflected the lack of a
253 chiasmata and failure of crossover formation, which almost never occurs in wild-type animals (Dernburg
254 et al., 1998; Yu et al., 2016). When exposed to 400 µM cisplatin, both *fcd-2* single mutants and *fcd-2; let-*
255 *418* double mutants suffered a significant deterioration in oocyte quality ($P < 0.04$ for both comparisons,
256 Fisher's exact test) (Fig. 3B). Each mutant produced oocytes with more than six DAPI bodies, and *fcd-2;*
257 *let-418* double mutants also produced an oocyte with only three DAPI bodies (Fig. 3F). Although
258 exposure to cisplatin did not induce a statistically significant change in wild-type and *let-418* single
259 mutants ($P > 0.5$ for both comparisons, Fisher's exact test), both genotypes produced oocyte classes that
260 were never observed in unexposed controls (Fig. 3E, F and Table S2).
261 When compared to either single mutant, *fcd-2; let-418* double mutants were more affected by
262 cisplatin exposure ($P < 0.003$ for both comparisons, Fisher's exact test). This difference was driven by
263 oocytes with both more and fewer DAPI bodies: *fcd-2; let-418* double mutants produced more nuclei
264 with four or fewer DAPI bodies, but also nuclei with seven to ten DAPI bodies, indicating a severe
265 disruption in crossover formation (Fig. 3F). Given our findings for mitotic DSBs, where the double
266 mutant phenocopied the *let-418* single mutant (Fig. 1 and Fig. 2), we were surprised to see that
267 diakinesis DAPI body number was significantly more affected in *fcd-2; let-418* double mutants than in
268 *let-418* single mutants. However, both the double mutant and *let-418* single mutant produced the rare
269 category of nuclei with three DAPI bodies (Fig. 3F). The severe reduction in DAPI bodies indicated that at
270 least half of the *C. elegans* genome has experienced chromosomal fusions, a phenotype that was also
271 previously observed in mutants missing both CHD paralogs (Turcotte et al., 2018).
272 Like cisplatin, 10 mM hydroxyurea also induced aneuploidy during diakinesis (Fig. 3C, D and
273 Table S2). Although exposure to hydroxyurea did not cause a statistically significant change in wild-type
274 population or *fcd-2* single mutants ($P > 0.3$ for both comparisons, Fisher's exact test), both genotypes
275 produced oocyte classes that were never observed in unexposed controls (Fig. S1 and Table S2).
276 However, unlike what we observed after cisplatin exposure, we did not find that *fcd-2* single mutants
277 produced nuclei with more than six DAPI bodies after hydroxyurea exposure (Fig. 3D), indicating that
278 *fcd-2* mutants were more sensitive to cisplatin. Exposed *let-418* single mutants were significantly
279 affected compared to wild-type controls, producing oocytes with both more than seven and fewer than
280 four DAPI bodies, categories that were never observed in unexposed controls ($P < 0.006$, Fisher's exact
281 test).

282 Challenging *fcd-2; let-418* double mutants with hydroxyurea caused a large deterioration in
283 oocyte quality ($P < 0.009$, Fisher's exact test). Exposed *fcd-2; let-418* double mutants were significantly
284 more affected than either of the exposed single mutant controls ($P < 0.004$ for both comparisons,
285 Fisher's exact test). This decline in oocyte quality was partly driven by nuclei with more than six DAPI
286 bodies (sometimes as many as ten), a category only observed in exposed *fcd-2; let-418* double mutants
287 and *let-418* single mutants (Fig. S1B). Once again, the existence of nuclei with univalents indicates that
288 hydroxyurea also causes a severe failure of crossover formation or chromosome fragmentation (Fig.
289 S1B). Taken together, this assessment of diakinesis nuclei indicates that *fcd-2; let-418* double mutants
290 are more sensitive to interstrand crosslinks and stalled replication forks than either single mutant.
291
292 Mutagen exposure reduces embryonic survival of *let-418* mutants.
293 After having shown that LET-418 is necessary to repair exogenous DSBs during mitosis (Fig. 1
294 and 2) and prevent aneuploidy during diakinesis (Fig. 3), we next examined oocyte viability by assessing
295 embryonic survival (Fig. 4 and Table S3). To capture the impact of mutagen exposure during mitosis, we
296 assessed embryos 60 hours later, which were produced by mothers in their third day of adulthood
297 (Jaramillo-Lambert et al., 2007; Kessler and Yanowitz, 2014). As expected for aged mothers, unexposed
298 wild-type populations had an average embryonic survival of 96% (Fig. 4A). As a positive control for
299 cisplatin sensitivity, we examined *xpf-1 (tm2842)* mutants, which lack an endonuclease involved in the
300 DNA damage response (Ward et al., 2007). Unexposed *xpf-1* mutants have a lower average survival than
301 unexposed wild-type populations ($P < 0.007$, ANOVA), which is reduced even further by cisplatin in a
302 dose-dependent manner (Fig. S2B and Table S5) (Meier et al., 2014; Ward et al., 2007). Survival in the
303 remaining unexposed mutants did not significantly differ from wild-type populations ($P > 0.1$ for all
304 comparisons, ANOVA), although each mutant displayed more variability and lower averages across
305 replicates compared to wild-type: across both cisplatin and hydroxyurea experiments, *fcd-2* single
306 mutants averaged 86% survival, *let-418* single mutants averaged 77% survival, and *fcd-2; let-418* double
307 mutants averaged 75% survival (Table S3). When challenged with 400 µM cisplatin, embryonic survival
308 in wild-type populations was significantly reduced to 73% ($P < 0.04$, ANOVA). As expected for a positive
309 control, cisplatin exposure reduced *xpf-1* mutant survival more severely than in wild-type populations,
310 dropping survival to 39% ($P < 0.01$, ANOVA) (Fig. 4A).
311 Embryonic survival in exposed *fcd-2* single mutants was not significantly affected compared to
312 unexposed controls ($P > 0.8$, ANOVA) (Fig. 4A). Conversely, exposed *let-418* single mutants experienced
313 a significant decline in survival, down to 39% ($P < 0.0001$, ANOVA), a decrease 2.4 times more than wild-

314 type and similar to *xpf-1* mutants (Fig. 4A). We noted that cisplatin had a variable impact on *let-418*
315 mutant survival, across both technical and biological replicates. This observation was consistent with
316 previous variability observed in *let-418* mutants (Turcotte et al., 2018): some replicates were completely
317 unaffected, resembling unexposed controls, whereas others suffered complete embryonic lethality that
318 was never observed in wild-type or *xpf-1* positive controls. Again, the effects of cisplatin on embryonic
319 survival in *fcd-2; let-418* double mutants strongly resembled *let-418* single mutants (Fig. 4A). Exposed
320 *fcd-2; let-418* double mutants experienced a significant drop in survival down to 33% ($P < 0.0001$,
321 ANOVA). As seen in *let-418* single mutants, this reduction was 2.7 times more than wild-type and similar
322 to *xpf-1* positive controls. However, in one departure from *let-418* single mutants, we found that
323 cisplatin caused less variability in *fcd-2; let-418* double mutant survival, which had a distribution that
324 overlapped only the lower half of that observed in *let-418* single mutants (Fig. 4A).
325 We next challenged hermaphrodites with 10 mM hydroxyurea to assess the impact on
326 embryonic survival (Fig. 4B). As expected, this low dose of exposure did not significantly reduce survival
327 in wild-type populations or *fcd-2* single mutants ($P > 0.09$ for both comparisons, ANOVA) (Kim et al.,
328 2018). However, *let-418* single mutants were sensitive to hydroxyurea – embryonic survival dropped
329 from 76% in unexposed controls to 46% after exposure ($P < 0.0003$, ANOVA), a reduction 2.1 times more
330 than experienced by wild-type populations (Fig. 4B). Exposed *fcd-2; let-418* double mutants suffered
331 from an even greater decrease in survival, from 73% down to 36% ($P < 0.0001$, ANOVA), a reduction 2.8
332 times more than wild-type (Fig. 4B).
333 Finally, we challenged hermaphrodites with an additional mutagen, nitrogen mustard, which
334 creates both interstrand crosslinks and DNA-protein crosslinks (Fig. S4 and Table S5) (Povirk and Shuker,
335 1994). A low dose of 100 µM did not affect wild-type embryonic survival ($P > 0.9$, ANOVA), whereas a
336 higher dose of 150 µM significantly decreased wild-type survival to 52% ($P < 0.0001$, ANOVA) (Fig. S4).
337 The low 100 µM dose of nitrogen mustard decreased survival in both *let-418* and *fcd-2* single mutants (P
338 < 0.0001 for both comparisons, ANOVA) and the high 150 µM dose further reduced survival to 25% ($P <$
339 0.0001 for both comparisons, ANOVA). Nitrogen mustard affected *fcd-2; let-418* double mutants
340 similarly to each single mutant ($P > 0.6$ for all comparisons), with survival severely reduced to 10% by
341 the high 150 µM dose ($P < 0.0001$ compared to unexposed control, ANOVA) (Fig. S4). Taken together,
342 the impact of mutagen exposure on embryonic survival indicate that LET-418 is required to resolve
343 exogenous DNA lesions to maintain oocyte viability.
344
345 <u>LET-418's ATPase domain is necessary for its role in germline DSB repair.</u>

346 The protein sequences of *C. elegans* LET-418 and human CHD4 share extensive homology,
347 including three domains: an ATPase domain, a PHD finger domain, and a double chromodomain (Fig. 5A)
348 (Farnung et al., 2020; Käser-Pébernard et al., 2016; Passannante et al., 2010). Computational models of
349 CHD4 structure suggest that each domain has distinct functions: the ATPase domain slides nucleosomes
350 along DNA (Farnung et al., 2020), the PHD finger domains bind modified histones, and the
351 chromodomains primarily bind DNA (Bouazoune et al., 2002). Mutations discovered in human patients,
352 along with *in vitro* experiments of CHD4 activity, have implicated each of these domains in CHD4's
353 nucleosome remodeling activity (Farnung et al., 2020; Watson et al., 2012; Weiss et al., 2016), but the
354 impact of each domain has yet to be assessed *in vivo*. Because the kinetics of repair occur rapidly in
355 response to DNA lesions (Kochan et al., 2017; Nair et al., 2017), we hypothesized that LET-418's function
356 in the germline requires its ATPase domain to slide nucleosomes and expose the site of DNA damage.
357 Figures 1 through 4 of this paper relied on the canonical allele *let-418 (n3536)*, a point mutation
358 in the ATPase domain that is hypomorphic, but viable, at the normal maintenance temperature of 20°C
359 (Andersen et al., 2006; Turcotte et al., 2018). We engineered separation-of function deletion alleles in
360 the *let-418* gene using CRISPR-Cas9 (see Methods for details). We then assessed the number of embryos
361 produced throughout the entire laying period in each *let-418* mutant (a full brood), using the canonical
362 *n3536* allele as a positive control (Fig. 5A and Table S4). Consistent with previous studies, wild-type
363 mothers produced broods that averaged 303 embryos (Fig 5C). Strikingly, mutants that lack the ATPase
364 domain*, syb6818*, were completely sterile and produced no embryos (Fig. 5C). In these ATPase deletion
365 mutants, we also noted a high occurrence of protruding vulvae and a clear body due to the lack of a fully
366 proliferated germline (Fig. 5B). Conversely, mutants that lack the PHD finger domain, *syb6708*, produced
367 an average brood of 268 embryos, which was not significantly lower than wild-type broods ($P > 0.7$,
368 ANOVA). Consistent with previous reports, average broods of canonical *n3636* mutants were 219
369 embryos, which represents a significant reduction compared to wild-type broods ($P < 0.001$, ANOVA).
370 We also noted the variability in canonical *n3636* mutant broods: some mothers produced at wild-type
371 levels (~300 embryos), whereas others were completely sterile (McMurchy et al., 2017; Turcotte et al.,
372 2018).
373 Because LET-418 is also involved in development (Erdelyi et al., 2017; Passannante et al., 2010;
374 von Zelewsky et al., 2000), we assessed embryonic survival throughout the full laying period. Average
375 survival of canonical *n3636* mutants was 95%, which represented a slight but significant reduction
376 compared average wild-type survival of 99% ($P < 0.05$, ANOVA). Similar to what we observed with brood
377 size, embryonic survival was not affected by the *syb6708* PHD deletion (Fig. 5D). Finally, we were unable

378 to assess survival in *syb6818* ATPase deletion mutants, because all mothers examined were sterile (N =
379 20). Altogether, our findings support a model in which NuRD's role in DNA repair during oogenesis
380 specifically requires LET-418's ATPase activity.
381
382 **DISCUSSION**
383 The germline must preserve genome integrity for all future generations, a task that requires
384 extensive coordination between DNA repair machinery and local chromatin environments (Chen and
385 Tyler, 2022; Clouaire and Legube, 2019). At the site of DNA damage, chromatin landscapes help
386 orchestrate repair using either error-prone or error-free DSB repair pathways (Chen and Tyler, 2022).
387 Although the mechanisms of DNA repair have been well-described across species, the role of chromatin
388 remodelers remains poorly understood. In this study, we show that LET-418, the ATPase remodeling
389 subunit of NuRD, is required to maintain oocyte quality when genomes are challenged by exogenous
390 DNA damage. After exposure to cisplatin or hydroxyurea, mutants with reduced LET-418 activity
391 accumulate more mitotic DSBs (Fig. 1 and Fig. 2), generate more aneuploid oocytes (Fig. 3), and suffer
392 from reduced embryonic viability (Fig. 4 and Fig. 5) – phenotypes that strongly resemble those seen in
393 mutants defective for the FA repair pathway (Adamo et al., 2010; Gartner and Engebrecht, 2022; Lee et
394 al., 2010). When testing the genetic relationship between NuRD and the FA pathway, we showed that
395 *let-418* gene activity is epistatic to the FA gene *fcd-2*, which suggests that NuRD nucleosome remodeling
396 is necessary to allow proper functioning of the FA repair pathway.
397 LET-418/CHD4 has been implicated in biological functions that include maintaining repressive
398 chromatin states, repairing DNA damage, and defining cell fate during embryonic development (De Vaux
399 et al., 2013; Guerry et al., 2007; Käser-Pébernard et al., 2016; Kunert et al., 2009; Saudenova and Wicky,
400 2018; Turcotte et al., 2018; Unhavaithaya et al., 2002; von Zelewsky et al., 2000). In mammals, CHD4's
401 role in resisting DNA damage has led to its upregulation in multiple types of cancer: for example, in
402 glioblastoma, CHD4 overexpression is associated with poor prognosis, likely due to its role in promoting
403 DNA damage repair to assure cancer cell survival (Chudnovsky et al., 2014; McKenzie et al., 2019). Other
404 work in ovarian cancer cells, acute myeloid leukemia cells, and mammary cells has shown that depleting
405 CHD4 impairs homologous recombination and sensitizes tumorigenic cells to DNA damaging agents (Pan
406 et al., 2012; Polo et al., 2010; Sperlazza et al., 2015). Similarly, in *C. elegans*, mutations in LET-418 or its
407 paralog CHD3 prevent DSB repair throughout meiotic pachytene, suggesting that LET-418/CHD4's role is
408 highly conserved across taxa (Turcotte et al., 2018).

409 Our work identifies a new role for LET-418/CHD4 in response to genotoxic threats – in the
410 absence of LET-418's ATPase activity, mutants cannot repair exogenous DNA damage incurred during
411 mitosis, which ultimately reduces gamete viability and impairs organismal survival. In germlines, LET-418
412 is associated with other heterochromatin factors that work with small RNA pathways to silence
413 repetitive elements and protect the genome (McMurchy et al., 2017). The DSB repair defects observed
414 in *let-418* mutants may be caused by disruptions in heterochromatin formation or maintenance, leading
415 to higher sensitivity to DNA damaging agents. A similar effect has been observed with the loss of
416 another core component of NuRD, RBBP4 (LIN-53 in *C. elegans*), which sensitizes cells to DNA damaging
417 agents by establishing a permissive chromatin environment and downregulating RAD51 expression
418 (Kitange et al., 2016).
419 We propose that LET-418 and NuRD are required during at least two points in gametogenesis: to
420 repair exogenous damage accumulated in mitosis and to resolve endogenous DSBs formed during
421 meiosis (this study and Turcotte et al., 2018). In the absence of LET-418 or NuRD activity, mitotic
422 damage persists as nuclei enter meiosis, contributing to the increase of DSBs observed in pachytene
423 (Turcotte et al., 2018). In meiosis, the FA pathway repairs DNA damage caused by replication fork
424 stalling or interstrand crosslinks – after the lesion is recognized, FA component FANCD2 is mono-
425 ubiquitinated and recruited to the lesion, where it mediates a conversion to DSBs and repair by
426 homologous recombination (Ceccaldi et al., 2016; Niraj et al., 2019).
427 Cytological experiments show that FA components, including FCD-2/FANCD2, are recruited to
428 DNA lesions to mediate repair in the mitotic region of the germline (Collis et al., 2006; Kim et al., 2018;
429 Lee et al., 2010). Our results are consistent with FCD-2 playing a role in resolving mitotic DSBs – exposed
430 *fcd-2* single mutants generated aneuploid oocytes that were never observed in wild-type populations:
431 some had chromosome fusions, whereas others experienced crossover failure (Fig. 3 and Fig. S1). These
432 defects represent genomic instability that is a consistent hallmark of defects with the FA pathway, and is
433 even used to diagnose human patients for Fanconi anemia (Adamo et al., 2010, 2010; Auerbach, 2009;
434 De Winter and Joenje, 2009; Lee et al., 2007; Rageul and Kim, 2020). However, we were surprised to find
435 that embryonic viability in *fcd-2* mutants was not affected by exposure to either cisplatin or hydroxyurea
436 (Fig. 4), since others have previously reported a cisplatin sensitivity in this mutant background (Adamo
437 et al., 2010; Collis et al., 2006; Germoglio et al., 2020). After examining the timing of exposure and
438 recovery used in those studies, we realized that they primarily assessed how damage induced during
439 late pachytene affected embryonic survival (Jaramillo-Lambert et al., 2007; Kessler and Yanowitz, 2014).
440 In contrast, we used a time course that allowed us to examine the effects of damage induced earlier

441 during mitosis. Altogether, our results suggest that FCD-2 and the FA pathway are involved in repairing
442 exogenous DSBs, but may not be the sole, or even the main, repair pathway at this point in
443 gametogenesis. However, in the later stages of meiotic prophase, all DSBs must be resolved before
444 chromosome segregation. Therefore, as nuclei approach diplotene, they rely on alternative error-prone
445 DSB repair pathways like NHEJ to resolve remaining DSBs (Macaisne et al., 2018; Smolikov et al., 2007).
446 These pathways usually result in non-crossovers and disruption of chiasmata formation, or can generate
447 chromosome translocations or fusions (Gartner and Engebrecht, 2022); we observed both outcomes in
448 diakinesis nuclei of *let-418* mutants.
449 We have also demonstrated that LET-418's activity is epistatic to that of FCD-2 and the FA
450 pathway – the *fcd-2; let-418* double mutant phenocopies the *let-418* single mutant when challenged by
451 exogenous DNA damage (Fig. 1, Fig. 2, and Fig. 4). When examining how mitotic DNA lesions affect
452 diakinesis DAPI body formation, we observed that *fcd-2; let-418* double mutants were more severely
453 affected by cisplatin and hydroxyurea than either single mutant (Fig. 3 and Fig. S1). Strikingly, double
454 mutant germlines contained classes of diakinesis nuclei that were only seen in one or the other single
455 mutant, suggesting an additive effect of losing both LET-418 and FCD-2 activity.
456 *C. elegans* LET-418 shares extensive homology with human CHD4, including an ATPase domain, a
457 PHD finger domain, and a double chromodomain (Käser-Pébernard et al., 2016; Passannante et al.,
458 2010). Computational models indicate that the ATPase domain repositions nucleosomes by sliding them
459 along DNA (Farnung et al., 2020). When examining human patient mutations identified in cancer or the
460 neurodevelopmental disorder Sifrim-Hitz-Weiss syndrome, we noticed that many missense mutations
461 occurred in the ATPase domain, indicating its importance for LET-418 and NuRD function. (Farnung et
462 al., 2020). To test the requirement for LET-418's ATPase activity *in vivo*, we engineered an endogenous
463 deletion of this domain (allele *syb6818*) and demonstrated that it is essential for LET-418's function in
464 the germline. ATPase deletion mutants were completely sterile (Fig. 5), and all homozygote mutants had
465 defective vulvas (Fig. 5B). Conversely, deletion of the PHD domain did not affect fertility or embryonic
466 survival, indicating that this domain is dispensable for LET-418's role in the germline. The ATPase
467 deletion phenotypes resemble those of *let-418* genetic null alleles, which were previously used to
468 characterize LET-418's role in vulval development (Guerry et al., 2007; von Zelewsky et al., 2000). In
469 somatic tissues, LET-418 belongs to two distinct complexes that have a conserved role in maintaining
470 cell identity – in addition to NuRD, it is also found in MEC, which consists of LET-418, the histone
471 deacetylase HDA-1, and the Krüppel-like protein MEP-1 (Hou et al., 2020; Käser-Pébernard et al., 2016;
472 Pfefferli et al., 2014; Unhavaithaya et al., 2002). As part of these complexes, LET-418 has roles in

473 specifying vulval fate, embryonic and larval development, and defining lifespan (De Vaux et al., 2013;
474 Erdelyi et al., 2017; Guerry et al., 2007; Käser-Pébernard et al., 2014; Passannante et al., 2010;
475 Saudenova and Wicky, 2018; von Zelewsky et al., 2000). Further characterization of these deletion
476 strains will establish their impact outside of the germline.
477 Based on our results, we propose the following model. When replication forks are blocked or
478 stalled, NuRD's remodeling activity creates a permissive chromatin environment that allows for the
479 recruitment of FA pathway components, like FCD-2, to repair the damage via homologous
480 recombination. In the absence of NuRD-mediated remodeling, the FA pathway is unable to repair DNA
481 lesions, causing the accumulation of mitotic and meiotic DSBs and their eventual resolution by error-
482 prone pathways later in meiosis. However, it is not clear from our findings whether NuRD functions
483 entirely upstream of the full FA pathway, or whether it mediates an intermediate step during interstrand
484 crosslink repair. For example, it is possible that DNA lesions are first recognized by the FA component
485 FNCM-1 (which acts upstream of FCD-2), which then recruits NuRD to the site of damage. In summary,
486 we've shown that LET-418's nucleosome remodeling activity is necessary to resolve germline DSBs by
487 error-free pathways like the FA pathway. This work highlights the important role of local chromatin
488 landscapes in coordinating DNA damage repair pathways during gametogenesis.
489
490 **DATA AVAILIBILITY**
491 Strains are available upon request. The authors affirm that all data necessary for confirming the
492 conclusions of the article are present within the article, figures, and tables.
493
494 **ACKNOWLEDGEMENTS**
495 We thank Diana Libuda and Monica Colaiacovo for generously sharing reagents, Cori Cahoon for
496 immunofluorescence advice, and WormBase for gene and sequence information (Davis et al., 2022).
497 Strains were provided by the *Caenorhabditis* Genetics Center, which is funded by the National Institutes
498 of Health (NIH) through the Office of Research Infrastructure Programs (P40 OD010440).
499
500 **FUNDING**
501 D. A. was supported by a UMass Lowell KCS Science Scholarship. T. B. and K. F. were supported by
502 fellowships from the UMass Lowell River Hawk Scholars Academy. K. F. was supported by the Urban
503 Massachusetts LSAMP program, which is funded by the National Science Foundation (EES 2308724). T.B.
504 was supported by the Society for Developmental Biology through a Choose Development! fellowship,

which is funded by the NIH (R25HD105600). This work was supported by the NIH, with grants R15GM117479 and R15HD104115 to P.M.C. and grant R15GM144861 to T.W.L.

CONFLICT OF INTEREST

The authors declare no conflicts of interest.

REFERENCES

Achache, H., Falk, R., Lerner, N., Beatus, T., Tzur, Y.B., 2021. Oocyte aging is controlled by mitogen-activated protein kinase signaling. Aging Cell 20, e13386. https://doi.org/10.1111/acel.13386

Adamo, A., Collis, S.J., Adelman, C.A., Silva, N., Horejsi, Z., Ward, J.D., Martinez-Perez, E., Boulton, S.J., La Volpe, A., 2010. Preventing Nonhomologous End Joining Suppresses DNA Repair Defects of Fanconi Anemia. Molecular Cell 39, 25–35. https://doi.org/10.1016/j.molcel.2010.06.026

Allis, C.D., Jenuwein, T., 2016. The molecular hallmarks of epigenetic control. Nat Rev Genet 17, 487–500. https://doi.org/10.1038/nrg.2016.59

Alpi, A., Pasierbek, P., Gartner, A., Loidl, J., 2003. Genetic and cytological characterization of the recombination protein RAD-51 in *Caenorhabditis elegans*. Chromosoma 112, 6–16. https://doi.org/10.1007/s00412-003-0237-5

Ananthaswamy, D., Croft, J.C., Woozencroft, N., Lee, T.W., 2022. *C. elegans* Gonad Dissection and Freeze Crack for Immunofluorescence and DAPI Staining. JoVE 64204. https://doi.org/10.3791/64204

Andersen, E.C., Lu, X., Horvitz, H.R., 2006. *C. elegans* ISWI and NURF301 antagonize an Rb-like pathway in the determination of multiple cell fates. Development 133, 2695–2704. https://doi.org/10.1242/dev.02444

Andux, S., Ellis, R.E., 2008. Apoptosis Maintains Oocyte Quality in Aging *Caenorhabditis elegans* Females. PLoS Genet 4, e1000295. https://doi.org/10.1371/journal.pgen.1000295

Auerbach, A.D., 2009. Fanconi anemia and its diagnosis. Mutation Research/Fundamental and Molecular Mechanisms of Mutagenesis 668, 4–10. https://doi.org/10.1016/j.mrfmmm.2009.01.013

Auerbach, A.D., 1993. Fanconi anemia diagnosis and the diepoxybutane (DEB) test. Exp Hematol 21, 731–733.

Bailly, A., Gartner, A., 2011. *Caenorhabditis elegans* Radiation Responses, in: DeWeese, T.L., Laiho, M. (Eds.), Molecular Determinants of Radiation Response. Springer New York, New York, NY, pp. 101–123. https://doi.org/10.1007/978-1-4419-8044-1_5

Basta, J., Rauchman, M., 2015. The nucleosome remodeling and deacetylase complex in development and disease. Translational Research 165, 36–47. https://doi.org/10.1016/j.trsl.2014.05.003

Becker, P.B., Workman, J.L., 2013. Nucleosome Remodeling and Epigenetics. Cold Spring Harbor Perspectives in Biology 5, a017905–a017905. https://doi.org/10.1101/cshperspect.a017905

546 Bouazoune, K., Mitterweger, A., Längst, G., Imhof, A., Akhtar, A., Becker, P.B., 2002. The dMi-2
547 chromodomains are DNA binding modules important for ATP-dependent nucleosome
548 mobilization. The EMBO Journal 21, 2430–2440.
549 https://doi.org/10.1093/emboj/21.10.2430
550 Brenner, S., 1974. THE GENETICS OF *CAENORHABDITIS ELEGANS*. Genetics 77, 71–94.
551 https://doi.org/10.1093/genetics/77.1.71
552 Ceccaldi, R., Rondinelli, B., D'Andrea, A.D., 2016. Repair Pathway Choices and Consequences at
553 the Double-Strand Break. Trends in Cell Biology 26, 52–64.
554 https://doi.org/10.1016/j.tcb.2015.07.009
555 Chapman, J.R., Taylor, M.R.G., Boulton, S.J., 2012. Playing the End Game: DNA Double-Strand
556 Break Repair Pathway Choice. Molecular Cell 47, 497–510.
557 https://doi.org/10.1016/j.molcel.2012.07.029
558 Chen, Z., Tyler, J.K., 2022. The Chromatin Landscape Channels DNA Double-Strand Breaks to
559 Distinct Repair Pathways. Front. Cell Dev. Biol. 10, 909696.
560 https://doi.org/10.3389/fcell.2022.909696
561 Chudnovsky, Y., Kim, D., Zheng, S., Whyte, W.A., Bansal, M., Bray, M.-A., Gopal, S., Theisen,
562 M.A., Bilodeau, S., Thiru, P., Muffat, J., Yilmaz, O.H., Mitalipova, M., Woolard, K., Lee, J.,
563 Nishimura, R., Sakata, N., Fine, H.A., Carpenter, A.E., Silver, S.J., Verhaak, R.G.W.,
564 Califano, A., Young, R.A., Ligon, K.L., Mellinghoff, I.K., Root, D.E., Sabatini, D.M., Hahn,
565 W.C., Chheda, M.G., 2014. ZFHX4 Interacts with the NuRD Core Member CHD4 and
566 Regulates the Glioblastoma Tumor-Initiating Cell State. Cell Reports 6, 313–324.
567 https://doi.org/10.1016/j.celrep.2013.12.032
568 Clouaire, T., Legube, G., 2019. A Snapshot on the Cis Chromatin Response to DNA Double-
569 Strand Breaks. Trends in Genetics 35, 330–345.
570 https://doi.org/10.1016/j.tig.2019.02.003
571 Colaiácovo, M.P., MacQueen, A.J., Martinez-Perez, E., McDonald, K., Adamo, A., La Volpe, A.,
572 Villeneuve, A.M., 2003. Synaptonemal Complex Assembly in *C. elegans* Is Dispensable
573 for Loading Strand-Exchange Proteins but Critical for Proper Completion of
574 Recombination. Developmental Cell 5, 463–474. https://doi.org/10.1016/S1534-
575 5807(03)00232-6
576 Collis, S.J., Barber, L.J., Ward, J.D., Martin, J.S., Boulton, S.J., 2006. *C. elegans* FANCD2 responds
577 to replication stress and functions in interstrand cross-link repair. DNA Repair 5, 1398–
578 1406. https://doi.org/10.1016/j.dnarep.2006.06.010
579 Datta, A., Brosh Jr., R.M., 2019. Holding All the Cards—How Fanconi Anemia Proteins Deal with
580 Replication Stress and Preserve Genomic Stability. Genes 10, 170.
581 https://doi.org/10.3390/genes10020170
582 Davis, P., Zarowiecki, M., Arnaboldi, V., Becerra, A., Cain, S., Chan, J., Chen, W.J., Cho, J., Da
583 Veiga Beltrame, E., Diamantakis, S., Gao, S., Grigoriadis, D., Grove, C.A., Harris, T.W.,
584 Kishore, R., Le, T., Lee, R.Y.N., Luypaert, M., Müller, H.-M., Nakamura, C., Nuin, P.,
585 Paulini, M., Quinton-Tulloch, M., Raciti, D., Rodgers, F.H., Russell, M., Schindelman, G.,
586 Singh, A., Stickland, T., Van Auken, K., Wang, Q., Williams, G., Wright, A.J., Yook, K.,
587 Berriman, M., Howe, K.L., Schedl, T., Stein, L., Sternberg, P.W., 2022. WormBase in
588 2022—data, processes, and tools for analyzing *Caenorhabditis elegans*. Genetics 220,
589 iyac003. https://doi.org/10.1093/genetics/iyac003

590 De Massy, B., 2013. Initiation of Meiotic Recombination: How and Where? Conservation and
591 Specificities Among Eukaryotes. Annu. Rev. Genet. 47, 563–599.
592 https://doi.org/10.1146/annurev-genet-110711-155423
593 De Vaux, V., Pfefferli, C., Passannante, M., Belhaj, K., Von Essen, A., Sprecher, S.G., Müller, F.,
594 Wicky, C., 2013. The *Caenorhabditis elegans* LET-418/ Mi2 plays a conserved role in
595 lifespan regulation. Aging Cell 12, 1012–1020. https://doi.org/10.1111/acel.12129
596 De Winter, J.P., Joenje, H., 2009. The genetic and molecular basis of Fanconi anemia. Mutation
597 Research/Fundamental and Molecular Mechanisms of Mutagenesis 668, 11–19.
598 https://doi.org/10.1016/j.mrfmmm.2008.11.004
599 Erdelyi, P., Wang, X., Suleski, M., Wicky, C., 2017. A Network of Chromatin Factors Is Regulating
600 the Transition to Postembryonic Development in *Caenorhabditis elegans*. G3
601 Genes|Genomes|Genetics 7, 343–353. https://doi.org/10.1534/g3.116.037747
602 Farnung, L., Ochmann, M., Cramer, P., 2020. Nucleosome-CHD4 chromatin remodeler structure
603 maps human disease mutations. eLife 9, e56178. https://doi.org/10.7554/eLife.56178
604 Gartner, A., Engebrecht, J., 2022. DNA repair, recombination, and damage signaling. Genetics
605 220, iyab178. https://doi.org/10.1093/genetics/iyab178
606 Germoglio, M., Valenti, A., Gallo, I., Forenza, C., Santonicola, P., Silva, N., Adamo, A., 2020. In
607 vivo analysis of FANCD2 recruitment at meiotic DNA breaks in *Caenorhabditis elegans*.
608 Sci Rep 10, 103. https://doi.org/10.1038/s41598-019-57096-1
609 Guerry, F., Marti, C.-O., Zhang, Y., Moroni, P.S., Jaquiéry, E., Müller, F., 2007. The Mi-2
610 nucleosome-remodeling protein LET-418 is targeted via LIN-1/ETS to the promoter of
611 lin-39/Hox during vulval development in *C. elegans*. Developmental Biology 306, 469–
612 479. https://doi.org/10.1016/j.ydbio.2007.03.026
613 Hou, T., Cao, Z., Zhang, J., Tang, M., Tian, Y., Li, Y., Lu, X., Chen, Y., Wang, Hui, Wei, F.-Z., Wang,
614 L., Yang, Y., Zhao, Y., Wang, Z., Wang, Haiying, Zhu, W.-G., 2020. SIRT6 coordinates with
615 CHD4 to promote chromatin relaxation and DNA repair. Nucleic Acids Res 48, 2982–
616 3000. https://doi.org/10.1093/nar/gkaa006
617 Jaramillo-Lambert, A., Ellefson, M., Villeneuve, A.M., Engebrecht, J., 2007. Differential timing of
618 S phases, X chromosome replication, and meiotic prophase in the *C. elegans* germ line.
619 Developmental Biology 308, 206–221. https://doi.org/10.1016/j.ydbio.2007.05.019
620 Käser-Pébernard, S., Müller, F., Wicky, C., 2014. LET-418/Mi2 and SPR-5/LSD1 Cooperatively
621 Prevent Somatic Reprogramming of *C. elegans* Germline Stem Cells. Stem Cell Reports 2,
622 547–559. https://doi.org/10.1016/j.stemcr.2014.02.007
623 Käser-Pébernard, S., Pfefferli, C., Aschinger, C., Wicky, C., 2016. Fine-tuning of chromatin
624 composition and Polycomb recruitment by two Mi2 homologues during *C. elegans* early
625 embryonic development. Epigenetics & Chromatin 9, 39.
626 https://doi.org/10.1186/s13072-016-0091-3
627 Keeney, S., 2007. Spo11 and the Formation of DNA Double-Strand Breaks in Meiosis, in: Egel, R.,
628 Lankenau, D.-H. (Eds.), Recombination and Meiosis, Genome Dynamics and Stability.
629 Springer Berlin Heidelberg, Berlin, Heidelberg, pp. 81–123.
630 https://doi.org/10.1007/7050_2007_026
631 Kehle, J., 1998. dMi-2, a Hunchback-Interacting Protein That Functions in Polycomb Repression.
632 Science 282, 1897–1900. https://doi.org/10.1126/science.282.5395.1897

633 Kessler, Z., Yanowitz, J., 2014. Methodological considerations for mutagen exposure in *C.*
634 *elegans*. Methods 68, 441–449. https://doi.org/10.1016/j.ymeth.2014.04.011
635 Kim, H.-M., Beese-Sims, S.E., Colaiácovo, M.P., 2018. Fanconi Anemia FANCM/FNCM-1 and
636 FANCD2/FCD-2 Are Required for Maintaining Histone Methylation Levels and Interact
637 with the Histone Demethylase LSD1/SPR-5 in *Caenorhabditis elegans*. Genetics 209,
638 409–423. https://doi.org/10.1534/genetics.118.300823
639 Kim, H.-M., Colaiácovo, M.P., 2015. DNA Damage Sensitivity Assays in *Caenorhabditis elegans*.
640 Bio Protoc 5, e1487.
641 Kim, S., Peterson, S.E., Jasin, M., Keeney, S., 2016. Mechanisms of germ line genome instability.
642 Seminars in Cell & Developmental Biology 54, 177–187.
643 https://doi.org/10.1016/j.semcdb.2016.02.019
644 Kitange, G.J., Mladek, A.C., Schroeder, M.A., Pokorny, J.C., Carlson, B.L., Zhang, Y., Nair, A.A.,
645 Lee, J.-H., Yan, H., Decker, P.A., Zhang, Z., Sarkaria, J.N., 2016. Retinoblastoma Binding
646 Protein 4 Modulates Temozolomide Sensitivity in Glioblastoma by Regulating DNA
647 Repair Proteins. Cell Reports 14, 2587–2598.
648 https://doi.org/10.1016/j.celrep.2016.02.045
649 Kochan, J.A., Desclos, E.C.B., Bosch, R., Meister, L., Vriend, L.E.M., van Attikum, H., Krawczyk,
650 P.M., 2017. Meta-analysis of DNA double-strand break response kinetics. Nucleic Acids
651 Res 45, 12625–12637. https://doi.org/10.1093/nar/gkx1128
652 Kunert, N., Wagner, E., Murawska, M., Klinker, H., Kremmer, E., Brehm, A., 2009. dMec: a novel
653 Mi-2 chromatin remodelling complex involved in transcriptional repression. EMBO J 28,
654 533–544. https://doi.org/10.1038/emboj.2009.3
655 Kurhanewicz, N.A., Dinwiddie, D., Bush, Z.D., Libuda, D.E., 2020. Elevated Temperatures Cause
656 Transposon-Associated DNA Damage in C. elegans Spermatocytes. Current Biology 30,
657 5007-5017.e4. https://doi.org/10.1016/j.cub.2020.09.050
658 Lachaud, C., Moreno, A., Marchesi, F., Toth, R., Blow, J.J., Rouse, J., 2016. Ubiquitinated Fancd2
659 recruits Fan1 to stalled replication forks to prevent genome instability. Science 351,
660 846–849. https://doi.org/10.1126/science.aad5634
661 Lee, K.Y., Chung, K.Y., Koo, H.-S., 2010. The involvement of FANCM, FANCI, and checkpoint
662 proteins in the interstrand DNA crosslink repair pathway is conserved in *C. elegans*. DNA
663 Repair 9, 374–382. https://doi.org/10.1016/j.dnarep.2009.12.018
664 Lee, K.Y., Yang, I., Park, J.-E., Baek, O.-R., Chung, K.Y., Koo, H.-S., 2007. Developmental stage-
665 and DNA damage-specific functions of *C. elegans* FANCD2. Biochemical and Biophysical
666 Research Communications 352, 479–485. https://doi.org/10.1016/j.bbrc.2006.11.039
667 Luo, S., Kleemann, G.A., Ashraf, J.M., Shaw, W.M., Murphy, C.T., 2010. TGF-β and Insulin
668 Signaling Regulate Reproductive Aging via Oocyte and Germline Quality Maintenance.
669 Cell 143, 299–312. https://doi.org/10.1016/j.cell.2010.09.013
670 Macaisne, N., Kessler, Z., Yanowitz, J.L., 2018. Meiotic Double-Strand Break Proteins Influence
671 Repair Pathway Utilization. Genetics 210, 843–856.
672 https://doi.org/10.1534/genetics.118.301402
673 McKenzie, L.D., LeClair, J.W., Miller, K.N., Strong, A.D., Chan, H.L., Oates, E.L., Ligon, K.L.,
674 Brennan, C.W., Chheda, M.G., 2019. CHD4 regulates the DNA damage response and
675 RAD51 expression in glioblastoma. Sci Rep 9, 4444. https://doi.org/10.1038/s41598-
676 019-40327-w

677 McMurchy, A.N., Stempor, P., Gaarenstroom, T., Wysolmerski, B., Dong, Y., Aussianikava, D.,
678 Appert, A., Huang, N., Kolasinska-Zwierz, P., Sapetschnig, A., Miska, E.A., Ahringer, J.,
679 2017. A team of heterochromatin factors collaborates with small RNA pathways to
680 combat repetitive elements and germline stress. eLife 6, e21666.
681 https://doi.org/10.7554/eLife.21666
682 Meier, B., Cooke, S.L., Weiss, J., Bailly, A.P., Alexandrov, L.B., Marshall, J., Raine, K., Maddison,
683 M., Anderson, E., Stratton, M.R., Gartner, A., Campbell, P.J., 2014. *C. elegans* whole-
684 genome sequencing reveals mutational signatures related to carcinogens and DNA
685 repair deficiency. Genome Res. 24, 1624–1636. https://doi.org/10.1101/gr.175547.114
686 Nair, N., Shoaib, M., Sørensen, C.S., 2017. Chromatin Dynamics in Genome Stability: Roles in
687 Suppressing Endogenous DNA Damage and Facilitating DNA Repair. IJMS 18, 1486.
688 https://doi.org/10.3390/ijms18071486
689 Nakanishi, K., Yang, Y.-G., Pierce, A.J., Taniguchi, T., Digweed, M., D'Andrea, A.D., Wang, Z.-Q.,
690 Jasin, M., 2005. Human Fanconi anemia monoubiquitination pathway promotes
691 homologous DNA repair. Proc. Natl. Acad. Sci. U.S.A. 102, 1110–1115.
692 https://doi.org/10.1073/pnas.0407796102
693 Nalepa, G., Clapp, D.W., 2018. Fanconi anaemia and cancer: an intricate relationship. Nat Rev
694 Cancer 18, 168–185. https://doi.org/10.1038/nrc.2017.116
695 Niraj, J., Färkkilä, A., D'Andrea, A.D., 2019. The Fanconi Anemia Pathway in Cancer. Annu. Rev.
696 Cancer Biol. 3, 457–478. https://doi.org/10.1146/annurev-cancerbio-030617-050422
697 Pan, M.-R., Hsieh, H.-J., Dai, H., Hung, W.-C., Li, K., Peng, G., Lin, S.-Y., 2012. Chromodomain
698 Helicase DNA-binding Protein 4 (CHD4) Regulates Homologous Recombination DNA
699 Repair, and Its Deficiency Sensitizes Cells to Poly(ADP-ribose) Polymerase (PARP)
700 Inhibitor Treatment. Journal of Biological Chemistry 287, 6764–6772.
701 https://doi.org/10.1074/jbc.M111.287037
702 Passannante, M., Marti, C.-O., Pfefferli, C., Moroni, P.S., Kaeser-Pebernard, S., Puoti, A.,
703 Hunziker, P., Wicky, C., Müller, F., 2010. Different Mi-2 Complexes for Various
704 Developmental Functions in *Caenorhabditis elegans*. PLoS ONE 5, e13681.
705 https://doi.org/10.1371/journal.pone.0013681
706 Pfefferli, C., Müller, F., Jaźwińska, A., Wicky, C., 2014. Specific NuRD components are required
707 for fin regeneration in zebrafish. BMC Biol 12, 30. https://doi.org/10.1186/1741-7007-
708 12-30
709 Polo, S.E., Kaidi, A., Baskcomb, L., Galanty, Y., Jackson, S.P., 2010. Regulation of DNA-damage
710 responses and cell-cycle progression by the chromatin remodelling factor CHD4. EMBO J
711 29, 3130–3139. https://doi.org/10.1038/emboj.2010.188
712 Povirk, L.F., Shuker, D.E., 1994. DNA damage and mutagenesis induced by nitrogen mustards.
713 Mutat Res 318, 205–226. https://doi.org/10.1016/0165-1110(94)90015-9
714 Rageul, J., Kim, H., 2020. Fanconi anemia and the underlying causes of genomic instability.
715 Environ and Mol Mutagen 61, 693–708. https://doi.org/10.1002/em.22358
716 Raghunandan, M., Chaudhury, I., Kelich, S.L., Hanenberg, H., Sobeck, A., 2015. FANCD2, FANCJ
717 and BRCA2 cooperate to promote replication fork recovery independently of the
718 Fanconi Anemia core complex. Cell Cycle 14, 342–353.
719 https://doi.org/10.4161/15384101.2014.987614

720 Saudenova, M., Wicky, C., 2018. The Chromatin Remodeler LET-418/Mi2 is Required Cell Non-
721 Autonomously for the Post-Embryonic Development of *Caenorhabditis elegans*. JDB 7, 1.
722 https://doi.org/10.3390/jdb7010001
723 Sayers, E.W., Bolton, E.E., Brister, J.R., Canese, K., Chan, J., Comeau, D.C., Connor, R., Funk, K.,
724 Kelly, C., Kim, S., Madej, T., Marchler-Bauer, A., Lanczycki, C., Lathrop, S., Lu, Z., Thibaud-
725 Nissen, F., Murphy, T., Phan, L., Skripchenko, Y., Tse, T., Wang, J., Williams, R., Trawick,
726 B.W., Pruitt, K.D., Sherry, S.T., 2022. Database resources of the national center for
727 biotechnology information. Nucleic Acids Research 50, D20–D26.
728 https://doi.org/10.1093/nar/gkab1112
729 Scharf, A., Pohl, F., Egan, B.M., Kocsisova, Z., Kornfeld, K., 2021. Reproductive Aging in
730 *Caenorhabditis elegans*: From Molecules to Ecology. Front. Cell Dev. Biol. 9, 718522.
731 https://doi.org/10.3389/fcell.2021.718522
732 Schindelin, J., Arganda-Carreras, I., Frise, E., Kaynig, V., Longair, M., Pietzsch, T., Preibisch, S.,
733 Rueden, C., Saalfeld, S., Schmid, B., Tinevez, J.-Y., White, D.J., Hartenstein, V., Eliceiri, K.,
734 Tomancak, P., Cardona, A., 2012. Fiji: an open-source platform for biological-image
735 analysis. Nat Methods 9, 676–682. https://doi.org/10.1038/nmeth.2019
736 Schlacher, K., Wu, H., Jasin, M., 2012. A Distinct Replication Fork Protection Pathway Connects
737 Fanconi Anemia Tumor Suppressors to RAD51-BRCA1/2. Cancer Cell 22, 106–116.
738 https://doi.org/10.1016/j.ccr.2012.05.015
739 Smolikov, S., Eizinger, A., Hurlburt, A., Rogers, E., Villeneuve, A.M., Colaiácovo, M.P., 2007.
740 Synapsis-defective mutants reveal a correlation between chromosome conformation
741 and the mode of double-strand break repair during *Caenorhabditis elegans* meiosis.
742 Genetics 176, 2027–2033. https://doi.org/10.1534/genetics.107.076968
743 Sperlazza, J., Rahmani, M., Beckta, J., Aust, M., Hawkins, E., Wang, S.Z., Zu Zhu, S., Podder, S.,
744 Dumur, C., Archer, K., Grant, S., Ginder, G.D., 2015. Depletion of the chromatin
745 remodeler CHD4 sensitizes AML blasts to genotoxic agents and reduces tumor
746 formation. Blood 126, 1462–1472. https://doi.org/10.1182/blood-2015-03-631606
747 Stinson, B.M., Loparo, J.J., 2021. Repair of DNA Double-Strand Breaks by the Nonhomologous
748 End Joining Pathway. Annu. Rev. Biochem. 90, 137–164.
749 https://doi.org/10.1146/annurev-biochem-080320-110356
750 Tischkowitz, M., Ameziane, N., Waisfisz, Q., De Winter, J.P., Harris, R., Taniguchi, T., D'Andrea,
751 A., Hodgson, S.V., Mathew, C.G., Joenje, H., 2003. Bi-allelic silencing of the Fanconi
752 anaemia gene *FANCF* in acute myeloid leukaemia: *Short Report*. British Journal of
753 Haematology 123, 469–471. https://doi.org/10.1046/j.1365-2141.2003.04640.x
754 Tischkowitz, M.D., Morgan, N.V., Grimwade, D., Eddy, C., Ball, S., Vorechovsky, I., Langabeer, S.,
755 Stöger, R., Hodgson, S.V., Mathew, C.G., 2004. Deletion and reduced expression of the
756 Fanconi anemia FANCA gene in sporadic acute myeloid leukemia. Leukemia 18, 420–
757 425. https://doi.org/10.1038/sj.leu.2403280
758 Tong, J.K., Hassig, C.A., Schnitzler, G.R., Kingston, R.E., Schreiber, S.L., 1998. Chromatin
759 deacetylation by an ATP-dependent nucleosome remodelling complex. Nature 395,
760 917–921. https://doi.org/10.1038/27699
761 Tsui, V., Crismani, W., 2019. The Fanconi Anemia Pathway and Fertility. Trends in Genetics 35,
762 199–214. https://doi.org/10.1016/j.tig.2018.12.007

763 Turcotte, C.A., Sloat, S.A., Rigothi, J.A., Rosenkranse, E., Northrup, A.L., Andrews, N.P., Checchi,
764 P.M., 2018. Maintenance of Genome Integrity by Mi2 Homologs CHD-3 and LET-418 in
765 *Caenorhabditis elegans*. Genetics 208, 991–1007.
766 https://doi.org/10.1534/genetics.118.300686
767 Unhavaithaya, Y., Shin, T.H., Miliaras, N., Lee, J., Oyama, T., Mello, C.C., 2002. MEP-1 and a
768 Homolog of the NURD Complex Component Mi-2 Act Together to Maintain Germline-
769 Soma Distinctions in *C. elegans*. Cell 111, 991–1002. https://doi.org/10.1016/S0092-
770 8674(02)01202-3
771 von Zelewsky, T., Palladino, F., Brunschwig, K., Tobler, H., Hajnal, A., Müller, F., Brehm, A., 2000.
772 The *C. elegans* Mi-2 chromatin-remodelling proteins function in vulval cell fate
773 determination. Development 127, 5277–5284. https://doi.org/10.1242/dev.127.24.5277
774 Wade, P.A., Jones, P.L., Vermaak, D., Wolffe, A.P., 1998. A multiple subunit Mi-2 histone
775 deacetylase from Xenopus laevis cofractionates with an associated Snf2 superfamily
776 ATPase. Current Biology 8, 843–848. https://doi.org/10.1016/S0960-9822(98)70328-8
777 Wang, Y., Zhang, H., Chen, Y., Sun, Y., Yang, F., Yu, W., Liang, J., Sun, L., Yang, X., Shi, L., Li, R., Li,
778 Y., Zhang, Y., Li, Q., Yi, X., Shang, Y., 2009. LSD1 Is a Subunit of the NuRD Complex and
779 Targets the Metastasis Programs in Breast Cancer. Cell 138, 660–672.
780 https://doi.org/10.1016/j.cell.2009.05.050
781 Ward, J.D., Barber, L.J., Petalcorin, M.I., Yanowitz, J., Boulton, S.J., 2007. Replication blocking
782 lesions present a unique substrate for homologous recombination. EMBO J 26, 3384–
783 3396. https://doi.org/10.1038/sj.emboj.7601766
784 Watson, A.A., Mahajan, P., Mertens, H.D.T., Deery, M.J., Zhang, Wenchao, Pham, P., Du, X.,
785 Bartke, T., Zhang, Wei, Edlich, C., Berridge, G., Chen, Y., Burgess-Brown, N.A.,
786 Kouzarides, T., Wiechens, N., Owen-Hughes, T., Svergun, D.I., Gileadi, O., Laue, E.D.,
787 2012. The PHD and chromo domains regulate the ATPase activity of the human
788 chromatin remodeler CHD4. J Mol Biol 422, 3–17.
789 https://doi.org/10.1016/j.jmb.2012.04.031
790 Weiss, K., Terhal, P.A., Cohen, L., Bruccoleri, M., Irving, M., Martinez, A.F., Rosenfeld, J.A.,
791 Machol, K., Yang, Y., Liu, P., Walkiewicz, M., Beuten, J., Gomez-Ospina, N., Haude, K.,
792 Fong, C.-T., Enns, G.M., Bernstein, J.A., Fan, J., Gotway, G., Ghorbani, M., DDD Study, van
793 Gassen, K., Monroe, G.R., van Haaften, G., Basel-Vanagaite, L., Yang, X.-J., Campeau,
794 P.M., Muenke, M., 2016. De Novo Mutations in CHD4, an ATP-Dependent Chromatin
795 Remodeler Gene, Cause an Intellectual Disability Syndrome with Distinctive
796 Dysmorphisms. Am J Hum Genet 99, 934–941.
797 https://doi.org/10.1016/j.ajhg.2016.08.001
798 Whyte, W.A., Bilodeau, S., Orlando, D.A., Hoke, H.A., Frampton, G.M., Foster, C.T., Cowley,
799 S.M., Young, R.A., 2012. Enhancer decommissioning by LSD1 during embryonic stem cell
800 differentiation. Nature 482, 221–225. https://doi.org/10.1038/nature10805
801 Wilson, T.E., Grawunder, U., Lieber, M.R., 1997. Yeast DNA ligase IV mediates non-homologous
802 DNA end joining. Nature 388, 495–498. https://doi.org/10.1038/41365
803 Woodage, T., Basrai, M.A., Baxevanis, A.D., Hieter, P., Collins, F.S., 1997. Characterization of the
804 CHD family of proteins. Proc. Natl. Acad. Sci. U.S.A. 94, 11472–11477.
805 https://doi.org/10.1073/pnas.94.21.11472

806 Xue, Y., Wong, J., Moreno, G.T., Young, M.K., Côté, J., Wang, W., 1998. NURD, a Novel Complex
807 with Both ATP-Dependent Chromatin-Remodeling and Histone Deacetylase Activities.
808 Molecular Cell 2, 851–861. https://doi.org/10.1016/S1097-2765(00)80299-3
809 Youds, J.L., Barber, L.J., Boulton, S.J., 2009. *C. elegans*: A model of Fanconi anemia and ICL
810 repair. Mutation Research/Fundamental and Molecular Mechanisms of Mutagenesis
811 668, 103–116. https://doi.org/10.1016/j.mrfmmm.2008.11.007
812
813
814 **FIGURE LEGENDS**
815
816 **Figure 1: *let-418* mutants cannot repair mitotic DSBs when challenged with cisplatin.**
817 **(A, B)** Stacked histograms showing the percentage of nuclei with the indicated number of foci for
818 animals exposed to 0 µM of cisplatin (A) and 400 µM of cisplatin (B). Average number of foci per nucleus
819 is indicated under each genotype. For all genotypes, exposed populations were significantly different
820 from unexposed controls (not indicated on histogram, $P < 0.0001$ for all comparisons). Each condition
821 includes at least 2000 nuclei analyzed from 15 germlines across three biological replicates. (**C, D**)
822 Representative images of mitotic region nuclei in unexposed (C) and exposed (D) animals, with the distal
823 tip oriented to the left (as indicated by white asterisk). Germlines are stained for RAD-51 (in yellow) and
824 DAPI (in blue). Scale bar represents 2 µm. All statistical analyses were performed using a Kruskal-Wallis
825 test with Dunn's post test (ns = not significant, * $P < 0.05$, **** $P < 0.0001$). Summary statistics are
826 included in Table S1.
827
828 **Figure 2: *let-418* mutants cannot repair mitotic DSBs when challenged with hydroxyurea.**
829 **(A, B)** Stacked histograms showing the percentage of nuclei with the indicated number of foci for
830 animals exposed to 0 mM of hydroxyurea (A) and 10 mM of cisplatin (B). Average number of foci per
831 nucleus is indicated under each genotype. For all genotypes, exposed populations were significantly
832 different from unexposed populations (not shown on graph, $P < 0.0001$ for all comparisons). Each
833 condition includes at least 2000 nuclei analyzed from 15 germlines across three biological replicates. (**C,**
834 **D**) Representative images of mitotic region nuclei in unexposed (C) and exposed (D) animals, with the
835 distal tip oriented to the left (as indicated by white asterisk). Germlines are stained for RAD-51 (in
836 yellow) and DAPI (in blue). Scale bar represents 2 µm. All statistical analyses were performed using a
837 Kruskal-Wallis test with Dunn's post test (ns = not significant, * $P < 0.05$, **** $P < 0.0001$). Summary
838 statistics are included in Table S1.
839
840 **Figure 3: *let-418* mutants have poor oocyte quality due to mutagen induced mitotic DSBs.**

841 **(A, B, C, D)** Stacked histograms showing the percentage of nuclei with the indicated number of DAPI
842 bodies for animals exposed to 0 µM of cisplatin (A), 400 µM of cisplatin, 0 mM of hydroxyurea (C) and 10
843 mM of hydroxyurea (D). Each condition includes at least 100 nuclei analyzed from 27 germlines across
844 three biological replicates. **(E, F)** Representative images of -1 oocytes in animals exposed to 0 uM of
845 cisplatin (E) and 400 uM of cisplatin (F). See Fig. S1 for representative images of -1 oocytes exposed to
846 cisplatin. Germlines are stained with DAPI (in white). Scale bar represents 2 µm. All statistical analyses
847 were performed as a Fisher's exact test on number of DAPI bodies (* $P < 0.05$, ** $P < 0.01$, **** $P <$
848 0.0001). Summary statistics are included in Table S2.
849
850 **Figure 4: DNA damaging agents reduce embryonic viability in *let-418* mutants.**
851 (**A, B**) Percent survival of indicated genotypes with and without exposure to cisplatin (A) or hydroxyurea
852 (B); dose is indicated with triangle above genotype names, with cisplatin in salmon (0 µM and 400 µM)
853 and hydroxyurea in blue (0 mM and 10 mM). For all conditions in (A) N=125 and (B) N=150. Dark line
854 represents the mean and whiskers represent S.E.M. All statistical analyses were performed using a one-
855 way ANOVA with a Šídák correction (*$P < 0.05$, ** $P < 0.01$, *** $P < 0.001$, **** $P < 0.0001$). Summary
856 statistics and data are found in Table S3.
857
858 **Figure 5: The ATPase motor domain is necessary for LET-418 protein function in DSB repair. (A)** Protein
859 alignment of human CHD4 and *C. elegans* LET-418 homologs showing conserved domains. Primary
860 structural alignments were performed according to NCBI-predicted domains using UniProt. The location
861 of the canonical *n3536* allele is indicated with a line. (**B**) Images of young adult hermaphrodites. The
862 ATPase deletion *syb6818*, has a protruding vulva (pVulv) phenotype (arrow) and a lack of germline as
863 indicated by the white space in the body. Scale bar, 100 µm. (**C**) Total brood was assessed in wild-type
864 (gray), the canonical allele *n3536* (light pink), the PHD finger deletion mutant *syb6708* (magenta), and
865 the ATPase deletion mutant *syb6818* (blue). (**D**) Percent embryonic survival, with the exception of *let-*
866 *418(syb6818)* due to its complete sterility. For both graphs, dark line represents mean and whiskers
867 represent S.E.M. All statistical analyses were performed using ANOVA with a Šídák correction (*$P < 0.05$,
868 *** $P < 0.001$, **** $P < 0.0001$). Summary statistics are included in Table S4.
869
870 **Figure S1: let-418 mutants have poor oocyte quality due to hydroxyurea induced mitotic DSBs.** (**A, B**)
871 Representative images of -1 to -4 oocytes in unexposed (C) and exposed (D) animals. Germlines are
872 stained with DAPI (in white). Scale bar represents 2 µm. Summary statistics are included in Table S2.

873

874 **Figure S2: Cisplatin affects embryonic survival in a dose-dependent manner.**

875 (**A, B**) Mean percent survival of wild-type populations (gray) exposed to doses of cisplatin ranging from 0
876 µM to 700 µM (A) or 0 µM to 400 µM (B). Relative dose levels are indicated by the triangles under the X-
877 axis. (B) Examining the effects of cisplatin on *let-418* mutants (pink). *xpf-1* mutants (green) are included
878 as a positive control for cisplatin sensitivity. Whiskers represent S.E.M. For each condition, at least 25
879 broods were evaluated. Summary statistics are included in Table S5.

880

881 **Figure S3: Hydroxyurea affects embryonic survival in a dose-dependent manner.** Mean percent
882 survival of wild-type (gray) and *let-418* mutants (pink) exposed to increasing doses of hydroxyurea (from
883 0 mM to 10 mM, with relative levels indicated by the blue triangle under the X-axis). Whiskers represent
884 S.E.M. For each condition, at least 25 broods were evaluated. Summary statistics are included in Table
885 S5.

886

887 **Figure S4: Nitrogen mustard reduces embryonic survival in *let-418* and *fcd-2* mutants.** Percent survival
888 of indicated genotypes with and without exposure nitrogen mustard; brown triangles indicate dose (0
889 mM, 100 mM, and 150 mM). Dark line represents mean percent survival and whiskers represent S.E.M.
890 Statistical comparisons to wild-type at the same dose are indicated with asterisks above mutant data. All
891 statistical analyses were performed using ANOVA followed by Šídák's multiple comparisons (**$P < 0.01$,
892 *** $P < 0.001$, **** $P < 0.0001$). Summary statistics are included in Table S5.

FIGURES WITH LEGENDS

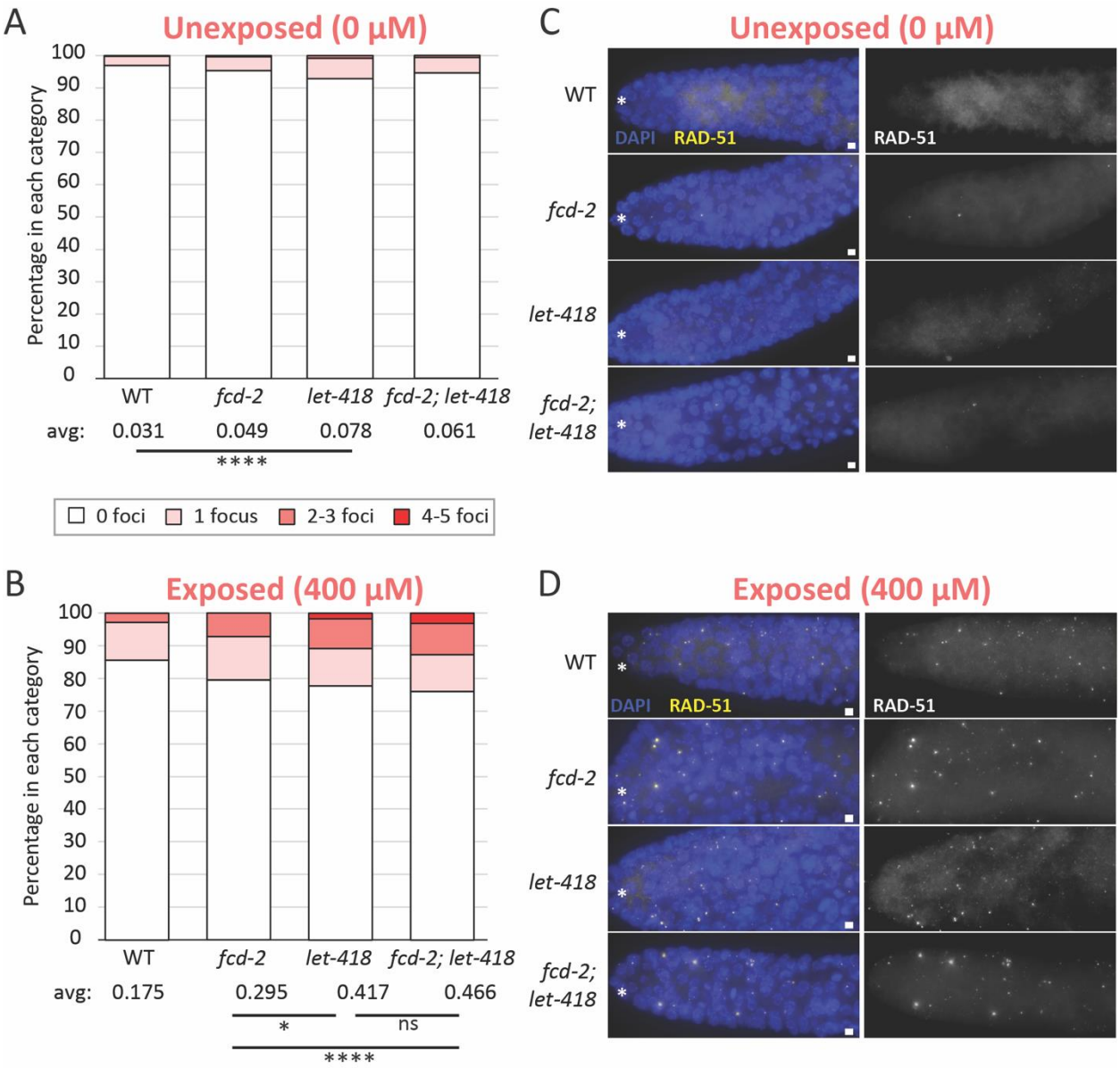

Figure 1: *let-418* mutants cannot repair mitotic DSBs when challenged with cisplatin.
(A, B) Stacked histograms showing the percentage of nuclei with the indicated number of foci for animals exposed to 0 µM of cisplatin (A) and 400 µM of cisplatin (B). Average number of foci per nucleus is indicated under each genotype. For all genotypes, exposed populations were significantly different from unexposed controls (not indicated on histogram, $P < 0.0001$ for all comparisons). Each condition includes at least 2000 nuclei analyzed from 15 germlines across three biological replicates. (**C, D**) Representative images of mitotic region nuclei in unexposed (C) and exposed (D) animals, with the distal tip oriented to the left (as indicated by white asterisk). Germlines are stained for RAD-51 (in yellow) and DAPI (in blue). Scale bar represents 2 µm. All statistical analyses were performed using a Kruskal-Wallis test with Dunn's post test (ns = not significant, * $P < 0.05$, **** $P < 0.0001$). Summary statistics are included in Table S1.

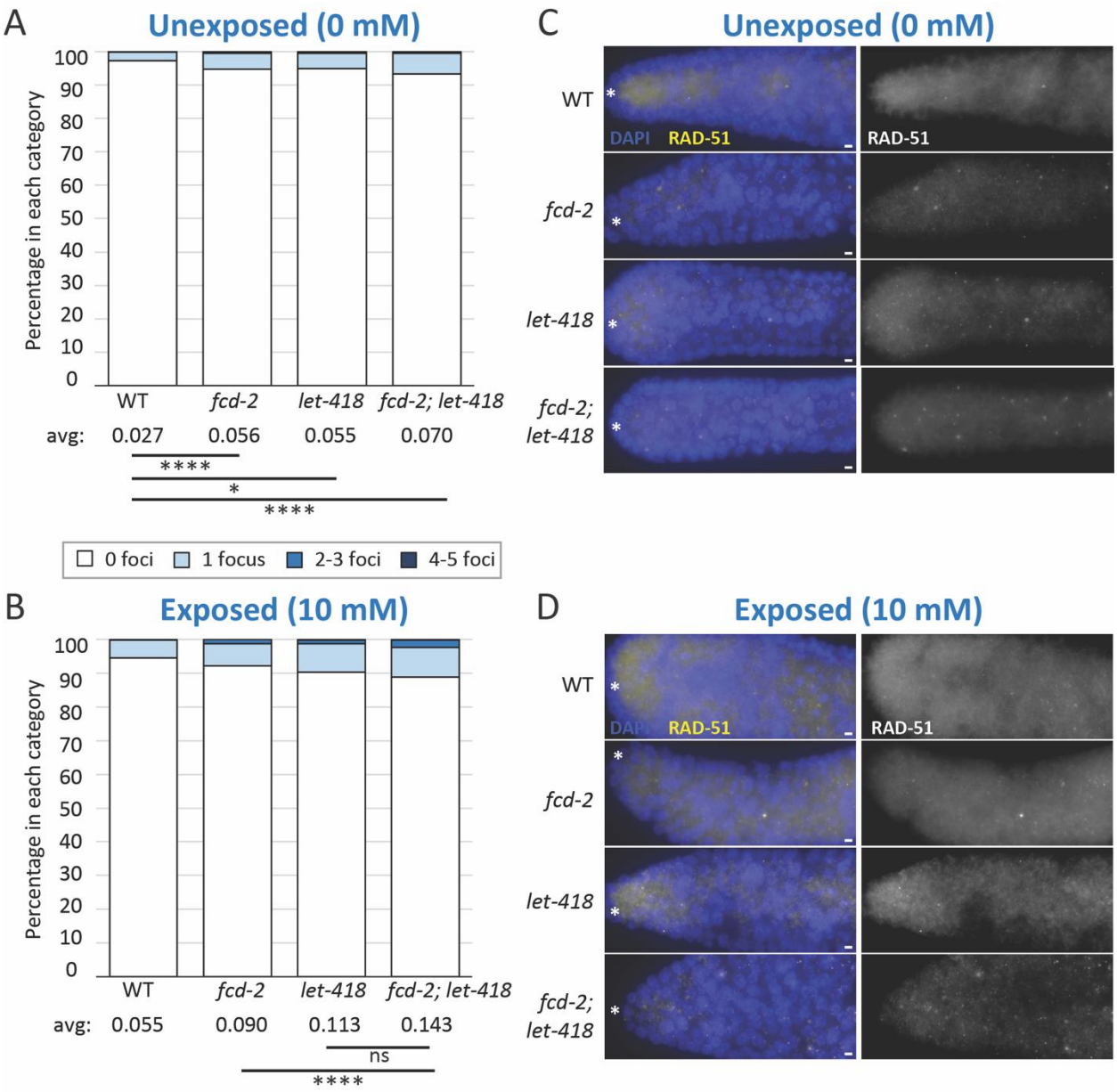

Figure 2: *let-418* mutants cannot repair mitotic DSBs when challenged with hydroxyurea.
(A, B) Stacked histograms showing the percentage of nuclei with the indicated number of foci for animals exposed to 0 mM of hydroxyurea (A) and 10 mM of cisplatin (B). Average number of foci per nucleus is indicated under each genotype. For all genotypes, exposed populations were significantly different from unexposed populations (not shown on graph, $P < 0.0001$ for all comparisons). Each condition includes at least 2000 nuclei analyzed from 15 germlines across three biological replicates. (**C, D**) Representative images of mitotic region nuclei in unexposed (C) and exposed (D) animals, with the distal tip oriented to the left (as indicated by white asterisk). Germlines are stained for RAD-51 (in yellow) and DAPI (in blue). Scale bar represents 2 µm. All statistical analyses were performed using a Kruskal-Wallis test with Dunn's post test (ns = not significant, * $P < 0.05$, **** $P < 0.0001$). Summary statistics are included in Table S1.

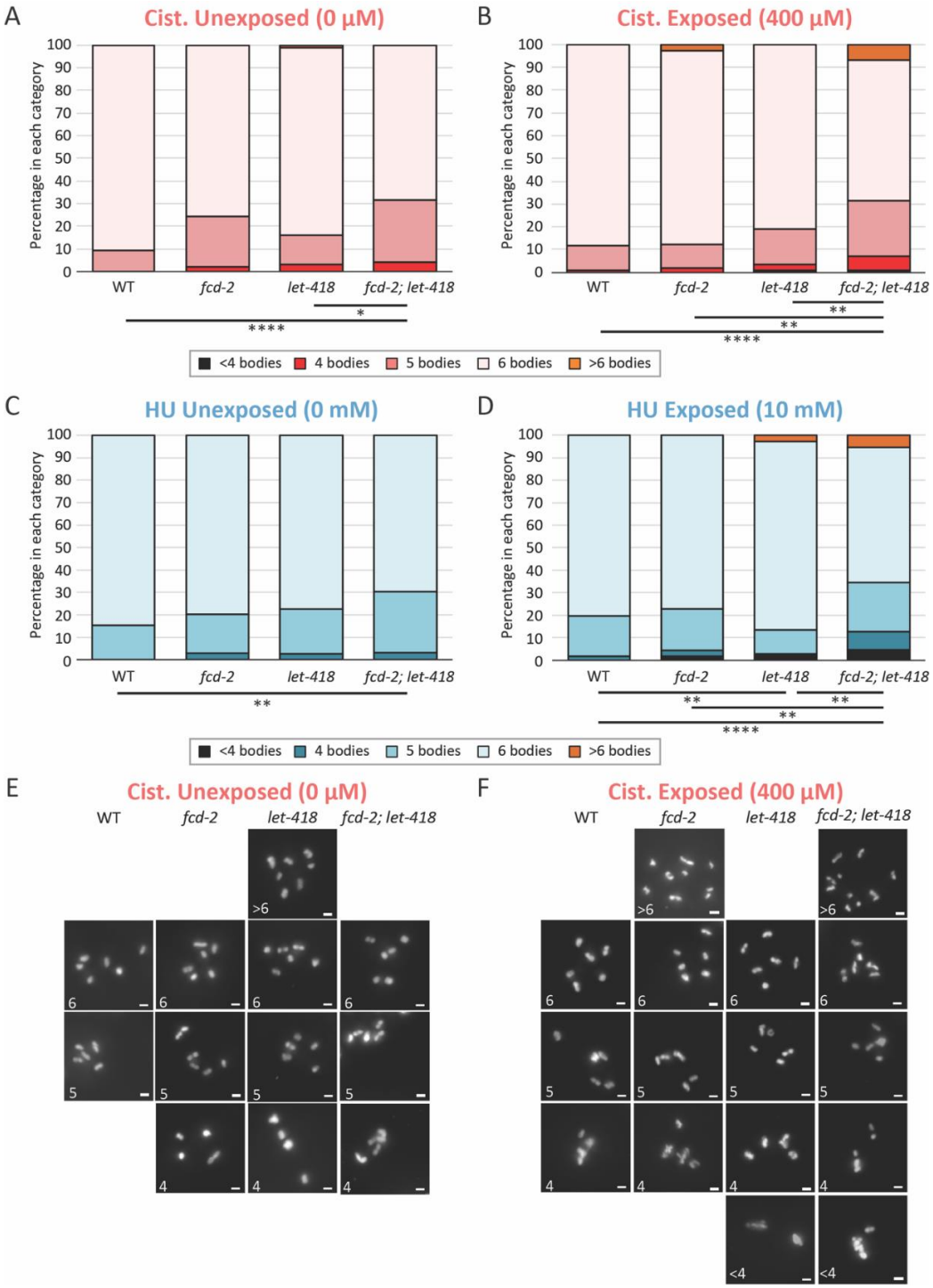

Figure 3: *let-418* mutants have poor oocyte quality due to mutagen induced mitotic DSBs.
(A, B, C, D) Stacked histograms showing the percentage of nuclei with the indicated number of DAPI bodies for animals exposed to 0 µM of cisplatin (A), 400 µM of cisplatin, 0 mM of hydroxyurea (C) and 10 mM of hydroxyurea (D). Each condition includes at least 100 nuclei analyzed from 27 germlines across three biological replicates. **(E, F)** Representative images of -1 oocytes in animals exposed to 0 uM of cisplatin (E) and 400 uM of cisplatin (F). See Fig. S1 for representative images of -1 oocytes exposed to cisplatin. Germlines are stained with DAPI (in white). Scale bar represents 2 µm. All statistical analyses were performed as a Fisher's exact test on number of DAPI bodies (* $P < 0.05$, ** $P < 0.01$, **** $P < 0.0001$). Summary statistics are included in Table S2.

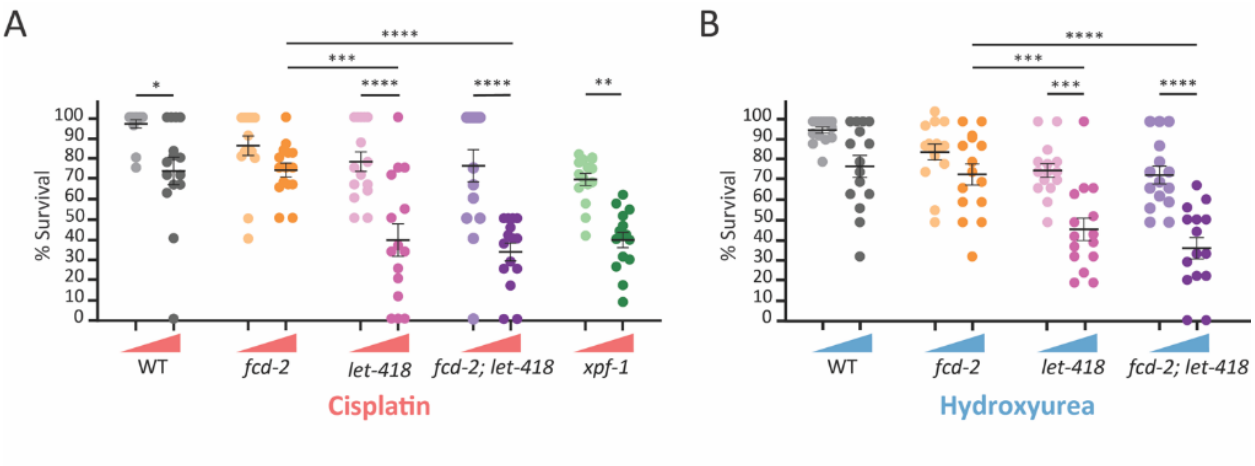

Figure 4: DNA damaging agents reduce embryonic viability in *let-418* mutants.
(**A, B**) Percent survival of indicated genotypes with and without exposure to cisplatin (A) or hydroxyurea (B); dose is indicated with triangle above genotype names, with cisplatin in salmon (0 µM and 400 µM) and hydroxyurea in blue (0 mM and 10 mM). For all conditions in (A) N=125 and (B) N=150. Dark line represents the mean and whiskers represent S.E.M. All statistical analyses were performed using a one-way ANOVA with a Šídák correction (*$P < 0.05$, ** $P < 0.01$, *** $P < 0.001$, **** $P < 0.0001$). Summary statistics and data are found in Table S3.

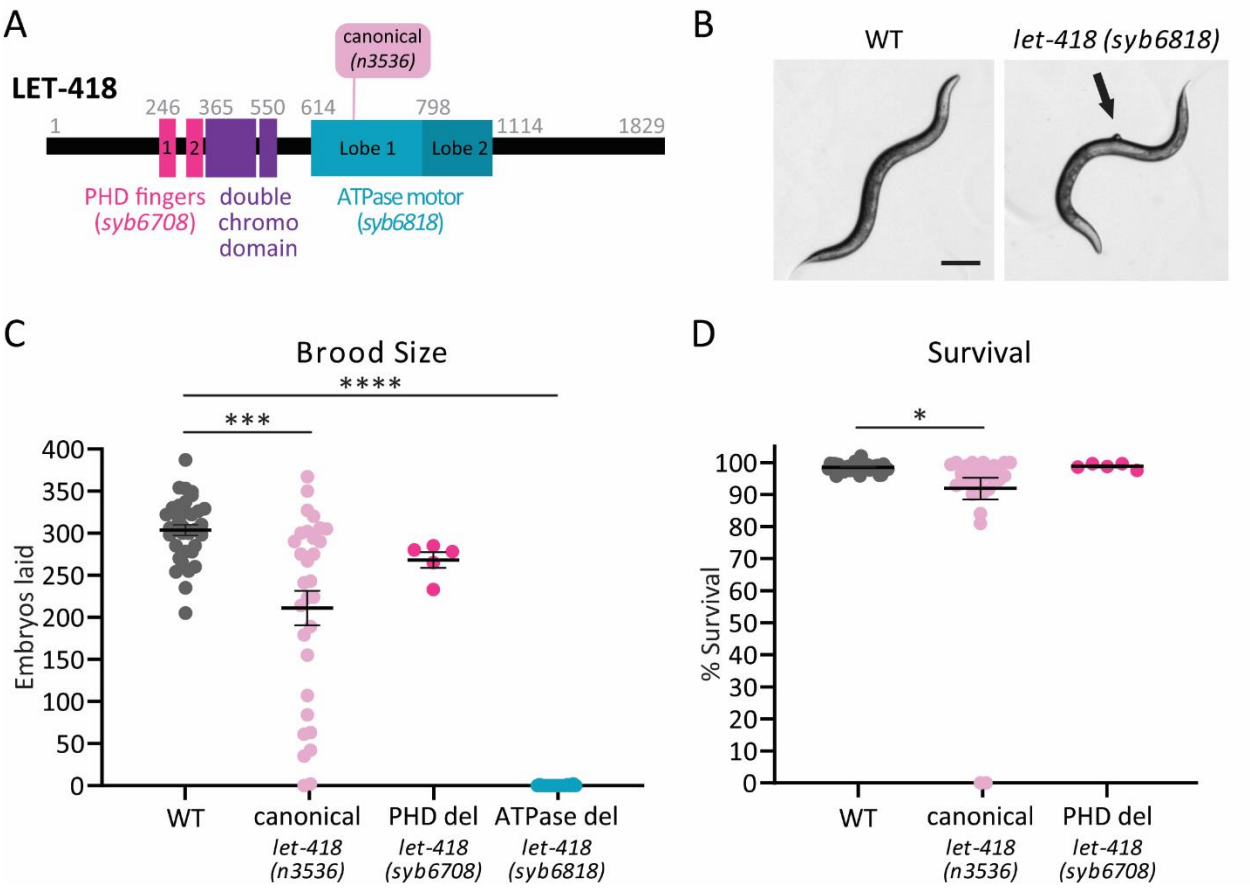

Figure 5: The ATPase motor domain is necessary for LET-418 protein function in DSB repair. (A) Protein alignment of human CHD4 and *C. elegans* LET-418 homologs showing conserved domains. Primary structural alignments were performed according to NCBI-predicted domains using UniProt. The location of the canonical *n3536* allele is indicated with a line. (**B**) Images of young adult hermaphrodites. The ATPase deletion *syb6818*, has a protruding vulva (pVulv) phenotype (arrow) and a lack of germline as indicated by the white space in the body. Scale bar, 100 µm. (**C**) Total brood was assessed in wild-type (gray), the canonical allele *n3536* (light pink), the PHD finger deletion mutant *syb6708* (magenta), and the ATPase deletion mutant *syb6818* (blue). (**D**) Percent embryonic survival, with the exception of *let-418(syb6818)* due to its complete sterility. For both graphs, dark line represents mean and whiskers represent S.E.M. All statistical analyses were performed using ANOVA with a Šídák correction (*$P < 0.05$, *** $P < 0.001$, **** $P < 0.0001$). Summary statistics are included in Table S4.

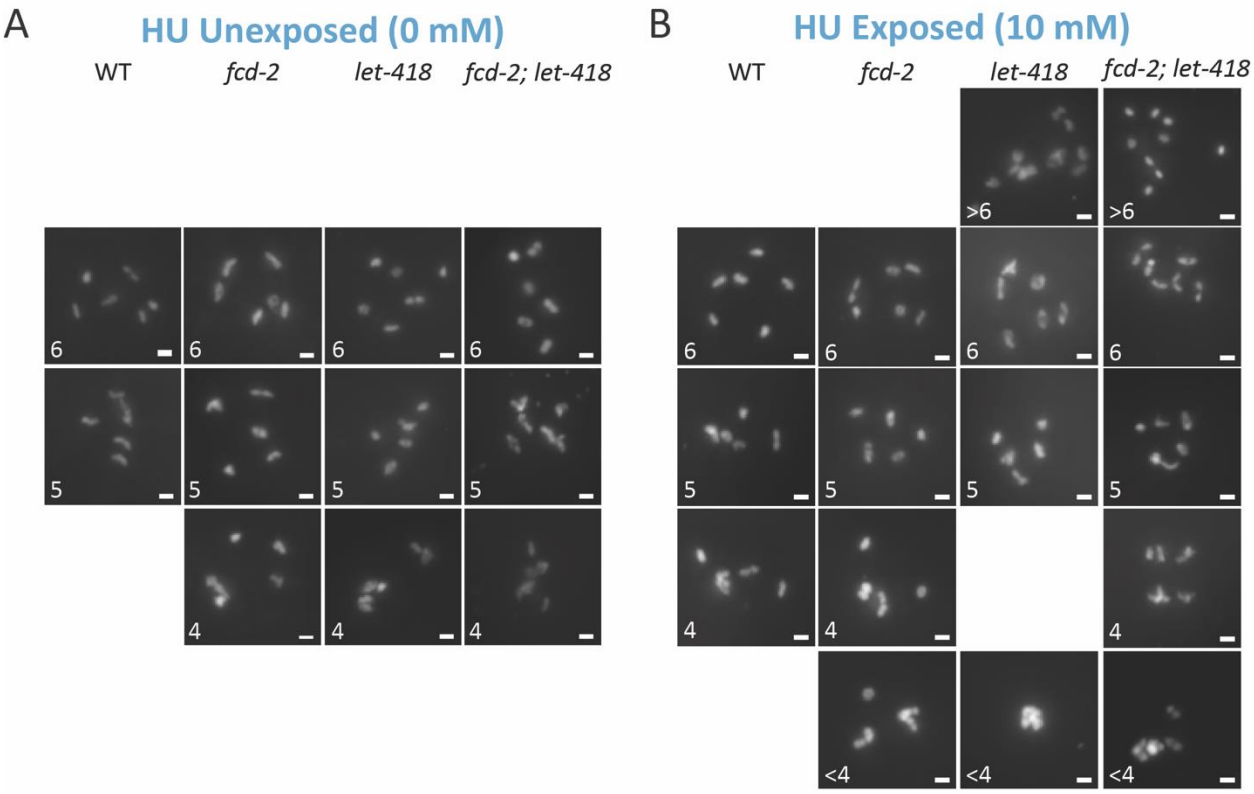

Figure S1: let-418 mutants have poor oocyte quality due to hydroxyurea induced mitotic DSBs. (**A, B**) Representative images of -1 to -4 oocytes in unexposed (C) and exposed (D) animals. Germlines are stained with DAPI (in white). Scale bar represents 2 µm. Summary statistics are included in Table S2.

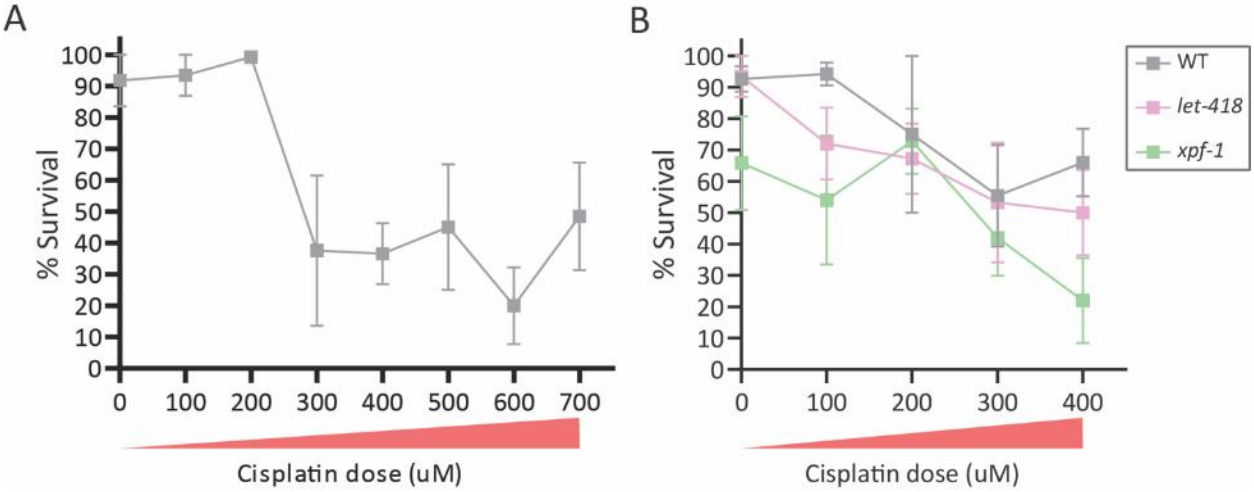

Figure S2: Cisplatin affects embryonic survival in a dose-dependent manner.
(**A, B**) Mean percent survival of wild-type populations (gray) exposed to doses of cisplatin of ranging from 0 µM to 700 µM (A) or 0 µM to 400 µM (B). Relative dose levels are indicated by the triangles under the X-axis. (B) Examining the effects of cisplatin on *let-418* mutants (pink). *xpf-1* mutants (green) are included as a positive control for cisplatin sensitivity. Whiskers represent S.E.M. For each condition, at least 25 broods were evaluated. Summary statistics are included in Table S5.

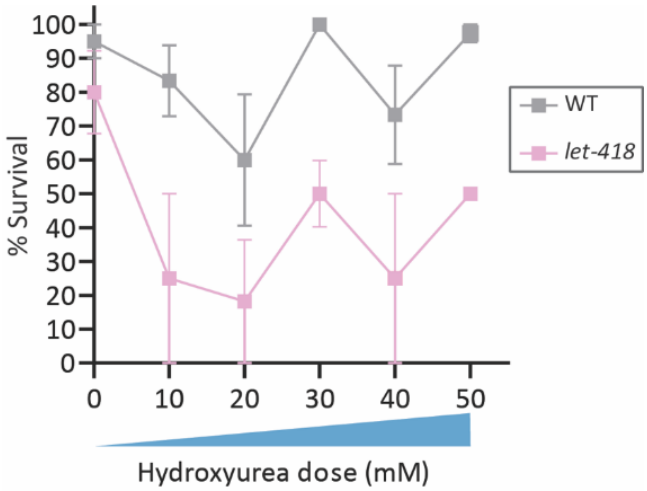

Figure S3: Hydroxyurea affects embryonic survival in a dose-dependent manner. Mean percent survival of wild-type (gray) and *let-418* mutants (pink) exposed to increasing doses of hydroxyurea (from 0 mM to 10 mM, with relative levels indicated by the blue triangle under the X-axis). Whiskers represent S.E.M. For each condition, at least 25 broods were evaluated. Summary statistics are included in Table S5.

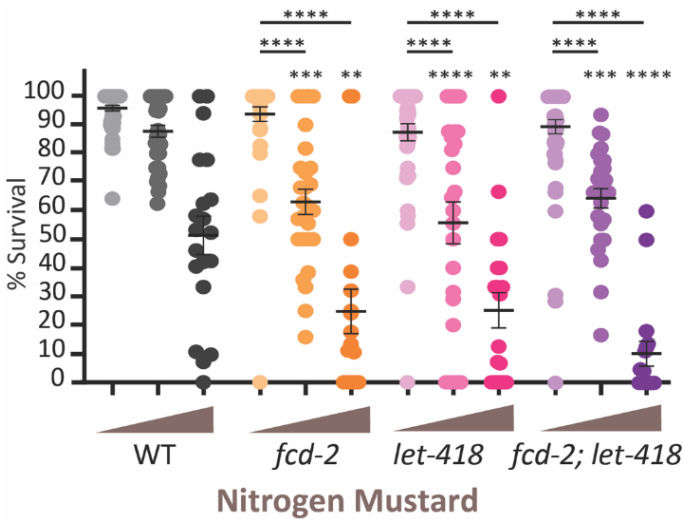

Figure S4: Nitrogen mustard reduces embryonic survival in *let-418* and *fcd-2* mutants. Percent survival of indicated genotypes with and without exposure nitrogen mustard; brown triangles indicate dose (0 mM, 100 mM, and 150 mM). Dark line represents mean percent survival and whiskers represent S.E.M. Statistical comparisons to wild-type at the same dose are indicated with asterisks above mutant data. All statistical analyses were performed using ANOVA followed by Šídák's multiple comparisons (**$P < 0.01$, *** $P < 0.001$, **** $P < 0.0001$). Summary statistics are included in Table S5.